



HAL
open science

Thick gradual sets and their computations: Application for determining the uncertain zone explored by an underwater robot

Reda Boukezzoula, Luc Jaulin, Benoit Desrochers, Laurent Foulloy

► To cite this version:

Reda Boukezzoula, Luc Jaulin, Benoit Desrochers, Laurent Foulloy. Thick gradual sets and their computations: Application for determining the uncertain zone explored by an underwater robot. Engineering Applications of Artificial Intelligence, 2021, 102, pp.104287. 10.1016/j.engappai.2021.104287 . hal-03224497

HAL Id: hal-03224497

<https://hal.science/hal-03224497v1>

Submitted on 24 May 2023

HAL is a multi-disciplinary open access archive for the deposit and dissemination of scientific research documents, whether they are published or not. The documents may come from teaching and research institutions in France or abroad, or from public or private research centers.

L'archive ouverte pluridisciplinaire **HAL**, est destinée au dépôt et à la diffusion de documents scientifiques de niveau recherche, publiés ou non, émanant des établissements d'enseignement et de recherche français ou étrangers, des laboratoires publics ou privés.



Distributed under a Creative Commons Attribution - NonCommercial 4.0 International License

Thick Gradual Sets and Their Computations: Application for Determining the Uncertain Zone Explored by an Underwater Robot

^(a)Reda Boukezzoula, ^(b)Luc Jaulin, ^(b)Benoit Desrochers, and ^(a)Laurent Foulloy

^(a)LISTIC–Université Savoie Mont Blanc, 5 Chemin de Bellevue, 74940 Annecy-le-Vieux, France

^(b)Lab–STICC, ENSTA-Bretagne, 2 rue François Verny; 29806 Brest, France

Abstract

This paper proposes a new concept of thick gradual sets (TGSs), which is based on the notions of thick sets (TSs) and gradual sets (GSs). A TS is an uncertain set, which is represented by a pair of crisp sets (CSs). These CSs represent the upper and lower bounds of the TS. Therefore, a TS can be considered as an interval of CSs. A GS is a CS, which is parameterized by a degree of pertinence and aims to increase the specificity of CSs. Furthermore, a TGS is an interval of GSs, i.e., a pair of lower and upper GSs. In situations when the constraint of monotonicity (consistency) is guaranteed, a GS becomes a type-1 fuzzy set (T1FS) and a TGS can be regarded as a thick fuzzy set (TFS). Moreover, a TFS, which is composed of lower and upper T1FS bounds, can be interpreted as a type-2 fuzzy set (T2FS). According to the TGS representation, this new approach offers an original concept for interpreting, manipulating, and computing some uncertain quantities that cannot be represented by GSs, T1FSs, and/or T2FSs. The potential applications of the TGS concept has been validated using application examples in the frameworks of solving fuzzy systems of equations and uncertain fuzzy regression and through a real-world application where the trajectory of an underwater robot is uncertain and cannot be precisely known because of disturbances induced by the environment. The proposed approach makes it possible to compute the uncertain zone explored by the underwater robot.

Keywords: Uncertain sets and thick sets (TSs), Gradual sets (GSs), Thick gradual sets (TGSs), Solving fuzzy systems of equations, Uncertain fuzzy regression, Zone explored by an underwater robot

1 Introduction

Usually, in set theory, an ordered crisp set (CS), which is denoted by \mathbb{X} , has its boundary known with certainty. However, in some practical applications, the boundary may become uncertain. To solve this problem, the concept of a thick set (TS) has been proposed in [18] and [19]. A TS is defined by two bounds. The lower bound is a CS, which contains all the certain elements. The upper bound is also a CS, which represents a set of plausible (perhaps possible) elements. The difference between these two CSs denotes the uncertainty (ignorance). This difference is called the penumbra [18].

From the methodological perspectives, the TS bounds can be viewed as lower and upper approximations in rough-set theory [1][54][55] (see [1] and [73] for a survey on rough-set theory, its variations, and its applications). Indeed, in rough-set theory, a CS is approximated using a pair of lower and upper CSs. Therefore, given the lower approximation (objects fully classified as \mathbb{X}) and upper approximation (objects possibly classified as \mathbb{X}), the boundary region of \mathbb{X} can be constructed. Thus, the uncertainty is characterized by the boundary region, which is interpreted as a rough set (objects that can neither be classified as \mathbb{X} nor its complement). It consists of objects that are not inside or outside \mathbb{X} . The boundary region denotes the difference between the upper and lower approximations. If the boundary region is empty, \mathbb{X} is considered as CS. In rough-set theory, information is often presented as a data table whose columns are labeled by attributes, the rows are labeled by objects of interest, and the table entries are attribute values. In its design, if the concept of TSs can be close to that of rough sets, their finality and field of application differ. In rough-set theory, the approximation of a CS by a pair of lower and upper CSs is elaborated using an equivalence relationship (an indiscernibility relation) defined by a set of attributes. In the TS approach, because lower bound \mathbb{X}^{inf} is included in upper bound \mathbb{X}^{sup} , any CS that belongs to the

penumbra is greater or equal to \mathbb{X}^{inf} and smaller or equal to \mathbb{X}^{sup} . In this sense, a TS can be viewed as an interval of CSs, which is represented by lower and upper CSs and denoted as $[\mathbb{X}] = [\mathbb{X}^{\text{inf}}, \mathbb{X}^{\text{sup}}]$. The penumbra, i.e., the difference between \mathbb{X}^{sup} and \mathbb{X}^{inf} , is a set of plausible but uncertain elements. Furthermore, in contrast to rough sets, the TS computations are implemented using interval-based arithmetic and solvers.

In the CS representation, the inclusion of an element to \mathbb{X} is certain, and that of an element that is outside it is impossible. The concept of gradual sets (GSs) has been proposed to remedy this lack of specificity [20]. It allows representation of the progressive belonging through a degree λ , which takes its values in the interval $[0, 1]$. This degree can be regarded as membership degrees of fuzzy sets, degrees of possibility, degrees of flexibility, etc. Thus, a GS can be regarded as a family of stacked CSs $\mathbb{X}(\lambda)$, $\lambda \in [0, 1]$. However, no nesting condition between CS $\mathbb{X}(\lambda)$ is required. A GS is defined by an assignment function associated with each degree of pertinence or flexibility λ of its CS $\mathbb{X}(\lambda)$. Therefore, the GS view enriches the representativeness of CSs by a vertical dimension. In situations where the constraint of monotonicity (consistency) is guaranteed, i.e., if $\lambda_1 > \lambda_2$, then $\mathbb{X}(\lambda_1) \subseteq \mathbb{X}(\lambda_2)$, and a GS becomes consonant and can be regarded as a type-1 fuzzy set (T1FS). In this case, CSs $\mathbb{X}(\lambda)$, $\lambda \in [0, 1]$ are λ -cuts. The literature is unanimous about the usefulness and importance of T1FSs, which have been the subject of countless works. However, some computations can lead to a family of stacked CSs, which are not nested according to the vertical λ dimension (e.g. [2], [7], [8], [20], and [40]). This situation provides GS its full meaning and its full usefulness. A discussion on the relationship between fuzzy sets and GSs can be found in [20].

With regard to TSs, which are introduced to deal with uncertain boundaries of CSs, thick GS (TGSs) are natural extension of TSs when gradual inclusion is considered. This new concept is based on the combination of the TS [18][19] and GS [20] notions. Therefore, a TGS is a family of stacked TSs $[\mathbb{X}(\lambda)] = [\mathbb{X}^{\text{inf}}(\lambda), \mathbb{X}^{\text{sup}}(\lambda)]$, $\lambda \in [0, 1]$. In a situation when the GS bounds $\mathbb{X}^{\text{inf}}(\lambda)$ and $\mathbb{X}^{\text{sup}}(\lambda)$ are consonant, they can be represented by T1FSs. In this framework, a TGS becomes a thick fuzzy set (TFS) and can be regarded as a type-2 fuzzy set (T2FS). Hence, the penumbra can be interpreted as the footprint of uncertainty (FOU) in the T2FS representation [46][51].

T1FSs cannot effectively model uncertainties [46]. In contrast to T1FSs, T2FSs can address uncertainties because their representation integrates two T1FSs. A T2FS is completely defined by two lower and upper T1FSs and is subjected to the inclusion constraint between them, i.e., lower T1FS \subset upper T1FS. In the T2FS representation, the FOU represents the blurring of a T1FS [46] and is delimited by the bounding lower and upper T1FSs. Therefore, the notion of uncertainty is introduced using the FOU concept. Over the past 30 years, interest in T2FSs has significantly increased owing to the works of Mendel et al. (e.g., [45], [47], [48], and [49]), Castillo et al. (e.g., [10], [11], and [12]), and many others. The undeniable potentialities of T2FSs have been demonstrated in various scopes, such as automatic control [10][11][44], multi-criteria decision making [5][39][57], aggregation operators [70][71], image processing, and pattern recognition [29][41]. T2FSs have demonstrated superior performance in many applications [72]. However, in some practical situations, the resulting uncertain quantities cannot be represented by T2FSs because their lower and/or upper bounds are not T1FSs but are instead GSs [2][8][40]. Consequently, the TGS concept finds its usefulness and its theoretical foundation to challenge this problem of uncertainty representation.

The motivation of the present study is twofold. The first motivation is to propose a tool to represent and compute some uncertain quantities that cannot be totally determined by CSs, T1FSs, GSs, and/or T2FSs. Therefore, we demonstrate a new methodology to manipulate uncertain GSs via TGSs using interval arithmetic and interval solvers. Furthermore, under the consistency constraint, a GS can be interpreted as a T1FS, and a TGS can be regarded as a T2FS. The proposed approach maintains the flexibility of the set-membership approaches and interval-arithmetic methods as major objectives. The second motivation is to validate the potentialities, usefulness, and feasibility of the

TGS concept through not only simulated applications such as solving fuzzy systems of equations (SoEs) and fuzzy regression problems but also using a real-world application where the objective is to model the zone explored by an underwater robot in an uncertain environment.

Section 2 presents the concepts and definitions of CSs, TSs, GSs, and TGSs and emphasizes their links to T1FSs and T2FSs. A simple example is used in this section to illustrate the concepts and processing. In Section 3, applications of the TGS approach to solve fuzzy SoEs and uncertain fuzzy regression are provided. Section 4 presents a real-world application of the TGS concept using an underwater robot. Finally, concluding remarks are presented in Section 5.

2 Concepts and definitions

2.1 Illustrative example

The concepts and definitions presented in this section are illustrated using a simple example of an autonomous vehicle that moves on a two-dimensional (2D) path. Its position is $\mathbf{x} = (x_1, x_2)$. The vehicle communicates with a transmitter located at position $\mathbf{m} = (m_1, m_2)$. When the vehicle is at a distance of less than 20 m to the transmitter, it detects its signal and can communicate with it. In this case, communication zone \mathbf{Z} is a circle with center \mathbf{m} and radius of 20 m, which is expressed as

$$\mathbf{Z} = \{\mathbf{x} \mid \|\mathbf{x} - \mathbf{m}\| \leq 20\}. \quad (1)$$

Fig. 1 shows the communication zone for $\mathbf{m} = (1, 3)$. When the vehicle is outside \mathbf{Z} , i.e., it is in $\bar{\mathbf{Z}}$, communication between the vehicle and transmitter is impossible. This basic condition will be explained further in the next subsections in relation to each new concept.

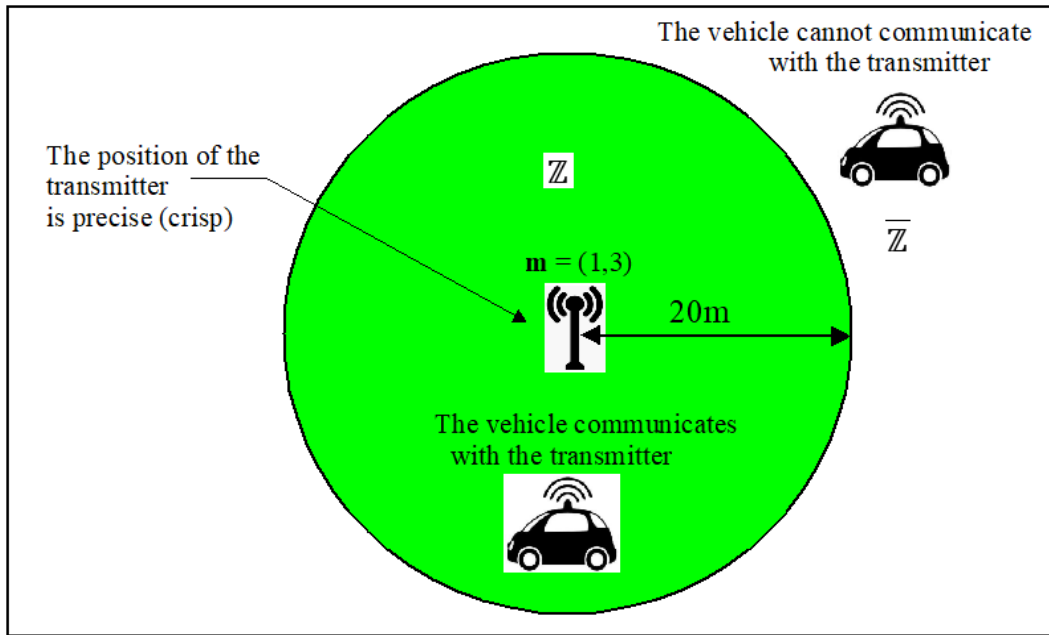


Fig. 1. Crisp communication zone for $\mathbf{m} = (1, 3)$.

2.2 CSs, crisp intervals (CIs), and boxes

Let \mathbb{X} be a crisp subset (often called CS for ease) of \square^n . CS \mathbb{X} simply represents the union of its contained singletons $\mathbf{x} = (x_1, \dots, x_n)$. The characteristic function of \mathbb{X} , $\mu_{\mathbb{X}} : \square^n \rightarrow \{0, 1\}$, is expressed as

$$\mu_{\mathbb{X}}(\mathbf{x}) = \begin{cases} 1 & \text{if } \mathbf{x} \in \mathbb{X}, \\ 0 & \text{if } \mathbf{x} \notin \mathbb{X}. \end{cases} \quad (2)$$

The elementary operations between two CSs \mathbb{X} and \mathbb{Y} , such as the intersection, union, and difference, are respectively expressed as follows:

$$\begin{cases} X \cap Y = \{a \mid a \in X \wedge a \in Y\}, \\ X \cup Y = \{a \mid a \in X \vee a \in Y\}, \\ X \setminus Y = \{a \mid a \in X \wedge a \notin Y\} = X \cap \bar{Y}, \end{cases} \quad (3)$$

where \wedge and \vee refer to the logical “and” and “or” operators, respectively, and \bar{Y} represents the complement of Y .

A crisp interval (CI) $[x]$ is a closed compact and bounded CS of \square such that $[x] = [x^-, x^+] = \{x \in \square \mid x^- \leq x \leq x^+\}$. A CI vector $[\mathbf{x}]$ (\mathbf{x} in bold) is called a box and is defined as the Cartesian product of n closed CIs, i.e.,

$$[\mathbf{x}] = [x_1] \times [x_2] \times \dots \times [x_n], \text{ where } [x_i] = [x_i^-, x_i^+], \text{ for } i = 1, \dots, n. \quad (4)$$

For example, Fig. 2 shows a 2D box, with $[\mathbf{x}] = [x_1] \times [x_2]$.

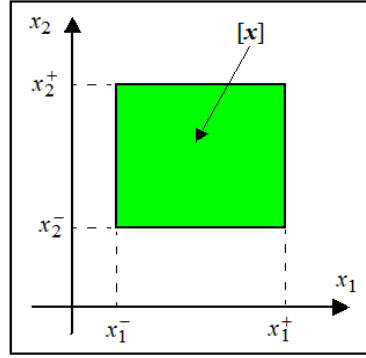


Fig. 2. 2D box $[\mathbf{x}] = [x_1] \times [x_2]$.

2.3 TSs, thick intervals (TIs), and thick boxes (TBs)

2.3.1 Definitions

Let $(P(\square^n), \subset)$ be the power set of \square^n equipped with inclusion order relationship \subset . Set $P(\square^n)$ is a complete lattice with respect to \subset (please refer to [18] and [19] for more details). TS $[[X]]$ of \square^n is an interval of $(P(\square^n), \subset)$ such that

$$[[X]] = [X^{\text{inf}}, X^{\text{sup}}] = \{X \in P(\square^n) \mid X^{\text{inf}} \subset X \subset X^{\text{sup}}\}. \quad (5)$$

TS $[[X]]$ is a sublattice of $(P(\square^n), \subset)$ [18][19] with lower and upper bounds X^{inf} and X^{sup} , respectively (see Fig. 3). Therefore, if $A \in [[X]]$ and $B \in [[X]]$, then $A \cap B \in [[X]]$, and $A \cup B \in [[X]]$. If $X^{\text{inf}} = X^{\text{sup}} = X$, then $[[X]]$ is a CS of \square^n , i.e., a singleton in $P(\square^n)$.

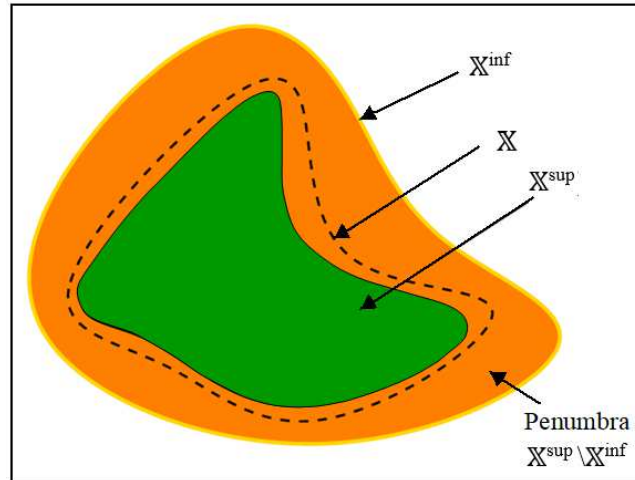


Fig. 3. Representation of TS $[[X]]$.

In contrast to CSs where only two logic values are used, in the TS representation, three logic values are necessary: “0” (False), “?” (Perhaps), and “1” (True). The fundamental logical operations

such as “and,” “or,” and “not” can be implemented using Kleene’s ternary logic [37][43] (see Fig. 4). Similar to a CS, the characteristic function of TS $\llbracket X \rrbracket$, $\mu_{\llbracket X \rrbracket}: \square^n \rightarrow \{0, ?, 1\}$, is defined as

$$\mu_{\llbracket X \rrbracket}(x) \mapsto \begin{cases} 1 & \text{if } x \in X^{\text{inf}}, \\ 0 & \text{if } x \notin X^{\text{sup}}, \\ ? & \text{otherwise.} \end{cases} \quad (6)$$

<i>and</i> (<i>a</i> , <i>b</i>)					<i>or</i> (<i>a</i> , <i>b</i>)					<i>not</i> (<i>a</i>)	
$a \wedge b$		b			$a \vee b$		b			a	\bar{a}
		0	?	1			0	?	1		
a	0	0	0	0	0	0	?	1	?	1	
	?	0	?	?	?	?	?	1	?	?	
	1	0	?	1	1	1	1	1	1	0	

Fig. 4. Operations *and*, *or*, and *not* using the Kleene’s ternary logic.

Equation (6) is an extension of the conventional characteristic function of a CS, as expressed in (2), of the TS case. In this context, the characteristic functions of TSs can be combined using the Kleene’s ternary operators. The arithmetical and logical operators among CSs can be extended to TSs [18][19][34]. For example, the intersection, union, and difference operators are respectively expressed as

$$\begin{cases} \llbracket X \rrbracket \cap \llbracket Y \rrbracket = \llbracket X^{\text{inf}} \cap Y^{\text{inf}}, X^{\text{sup}} \cap Y^{\text{sup}} \rrbracket, \\ \llbracket X \rrbracket \cup \llbracket Y \rrbracket = \llbracket X^{\text{inf}} \cup Y^{\text{inf}}, X^{\text{sup}} \cup Y^{\text{sup}} \rrbracket, \\ \llbracket X \rrbracket \setminus \llbracket Y \rrbracket = \llbracket X^{\text{inf}} \setminus Y^{\text{sup}}, X^{\text{sup}} \setminus Y^{\text{inf}} \rrbracket. \end{cases} \quad (7)$$

A TI is a special case of a TS such that $\llbracket x \rrbracket = \llbracket [x^{\text{inf}}], [x^{\text{sup}}] \rrbracket$, $[x^{\text{inf}}] \subset [x^{\text{sup}}]$ [see Fig. 5(a)]. If $[x^{\text{inf}}] = [x^{\text{sup}}] = [x]$, TI $\llbracket x \rrbracket$ becomes a CI, i.e., $\llbracket x \rrbracket = [x]$. Another representation of TIs that is based on the left and right CIs has been proposed [6]. These two representations are equivalent.

A TI vector $\llbracket \mathbf{x} \rrbracket = \llbracket [\mathbf{x}^{\text{inf}}], [\mathbf{x}^{\text{sup}}] \rrbracket$ (\mathbf{x} in bold) is known as a TB. Because $[x^{\text{inf}}]$ and $[x^{\text{sup}}]$ are boxes of \square^n , they can be expressed as the Cartesian product of n CIs [see Fig. 5(b) for a 2D TB], i.e.,

$$\begin{cases} [\mathbf{x}^{\text{inf}}] = [x_1^{\text{inf}}] \times [x_2^{\text{inf}}] \times \dots \times [x_n^{\text{inf}}], \\ [\mathbf{x}^{\text{sup}}] = [x_1^{\text{sup}}] \times [x_2^{\text{sup}}] \times \dots \times [x_n^{\text{sup}}]. \end{cases} \quad (8)$$

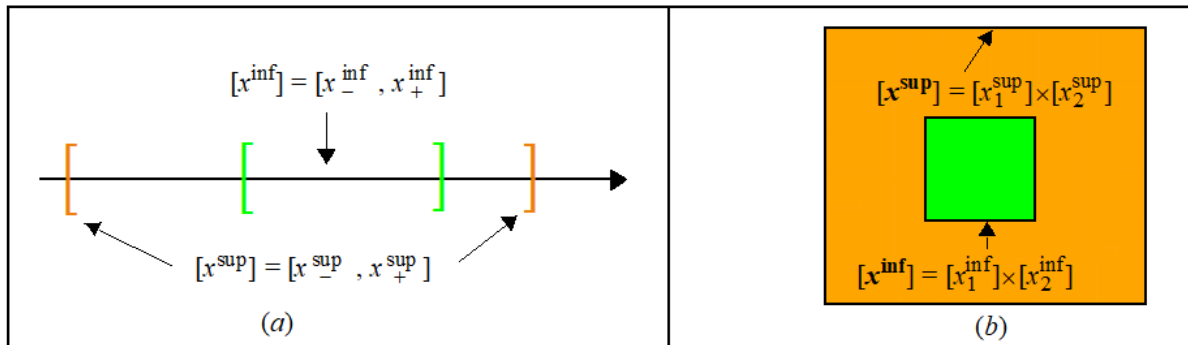


Fig. 5. Representations of TI and TB.

2.3.2 Illustration

Because of the possible presence of obstacles and disturbances induced by other networks, the autonomous vehicle locates the transmitter position with uncertainty, which is represented by a 2D box $\llbracket \mathbf{m} \rrbracket = \llbracket [m_1] \times [m_2] \rrbracket$. We need to note that this representation by a box is relatively poor. However,

it will be enriched later. Thus, two nested communication zones can coexist. The first one is defined by all positions \mathbf{x} of the vehicle where communication with the transmitter is certain regardless of its location \mathbf{m} in $[\mathbf{m}]$. The second one, which encompasses the first one, is the zone where the communication with the transmitter is plausible, i.e., at least one location \mathbf{m} in $[\mathbf{m}]$ exists where communication between the vehicle and transmitter is possible. If each zone is represented by a CS, their difference represents the uncertainty (ignorance) and is interpreted as the zone where communication between the vehicle and transmitter is plausible but not certain (perhaps possible). Let $A \subset X \times M$ be the constraint

$$A = \{(\mathbf{x}, \mathbf{m}) \in \square^4 \mid \|\mathbf{x} - \mathbf{m}\| \leq 20\} = \{(\mathbf{x}, \mathbf{m}) \in \square^4 \mid (x_1 - m_1)^2 + (x_2 - m_2)^2 \leq 400\}. \quad (9)$$

Constraint (9) is a four-dimensional CS that defines all positions $\mathbf{x} = (x_1, x_2) \in \square^2$ of the vehicle and all locations $\mathbf{m} = (m_1, m_2) \in \square^2$ of the transmitter such that the Euclidean distance ($\|\mathbf{x} - \mathbf{m}\|$) between \mathbf{x} and \mathbf{m} is ≤ 20 m. Because exact location $\mathbf{m} = (m_1, m_2)$ of the transmitter is located in box $[\mathbf{m}] = [m_1] \times [m_2]$, i.e., $m_1 \in [m_1]$ and $m_2 \in [m_2]$, communication zone \mathbb{Z} becomes uncertain, and we have $\mathbb{Z}^{\text{inf}} \subset \mathbb{Z} \subset \mathbb{Z}^{\text{sup}}$ where

$$\begin{cases} \mathbb{Z}^{\text{sup}} = \{\mathbf{x} \mid \exists \mathbf{m} \in [\mathbf{m}], \|\mathbf{x} - \mathbf{m}\| \leq 20\}, \\ \mathbb{Z}^{\text{inf}} = \{\mathbf{x} \mid \forall \mathbf{m} \in [\mathbf{m}], \|\mathbf{x} - \mathbf{m}\| \leq 20\}. \end{cases} \quad (10)$$

CS \mathbb{Z}^{inf} represents a certain zone, which consists of all points \mathbf{x} in \square^2 , where communication between the vehicle and transmitter is certain regardless of its location \mathbf{m} in $[\mathbf{m}]$. CS \mathbb{Z}^{sup} corresponds to the zone where communication between the vehicle and transmitter is plausible. Outside \mathbb{Z}^{sup} , communication is impossible. CS $\mathbb{Z}^{\text{sup}} \setminus \mathbb{Z}^{\text{inf}}$ represents the penumbra, which is an uncertain zone where communication is plausible but uncertain. The communication zone can be expressed as TS $[[\mathbb{Z}]] = [[\mathbb{Z}^{\text{inf}}, \mathbb{Z}^{\text{sup}}]]$. The bounds \mathbb{Z}^{inf} and \mathbb{Z}^{sup} can be computed from the projections on Ξ of the intersection of A with Cartesian product $X \times [\mathbf{m}]$

$$\begin{cases} \mathbb{Z}^{\text{sup}} = \text{proj}_X A \cap (X \times [\mathbf{m}]), \\ \mathbb{Z}^{\text{inf}} = \overline{\text{proj}_X \bar{A} \cap (X \times [\mathbf{m}])}, \end{cases} \quad (11)$$

where the bar symbol indicates the complement of the set under the bar.

For the sake of simplicity in representation, we consider the case where m_2 is constant, e.g., $m_2 = 0$, and can be omitted. Thus, we let $[\mathbf{m}] = [m_1] = [-10, 10]$. In this case, constraint (9) becomes

$$A = \{(\mathbf{x}, m_1) \in \square^3 \mid (x_1 - m_1)^2 + x_2^2 \leq 400\}. \quad (12)$$

This constraint is a cylinder in space (x_1, x_2, m_1) . Fig. 6(a) shows the envelope of the cylinder and two planes, which are the upper and lower bounds of Cartesian product $X \times [-10, 10]$. Figs. 6(b) and 7 show how \mathbb{Z}^{inf} and \mathbb{Z}^{sup} are obtained from the projections.

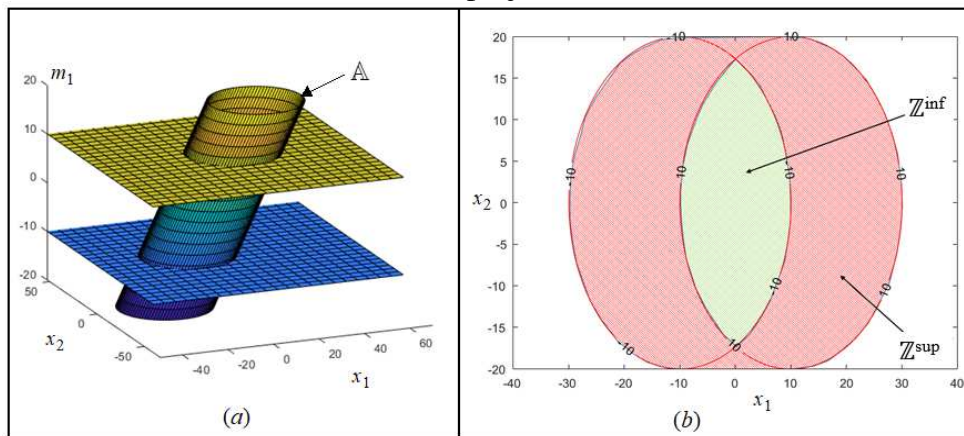


Fig. 6. Illustration of the projection principle.

Efficient computation of \mathbb{Z}^{inf} and \mathbb{Z}^{sup} can be performed using the method proposed in [33]. The main idea is to use interval computation to determine whether or not the projections of box $[\mathbf{x}] \times [\mathbf{m}] \subset X \times M$ belong to \mathbb{Z}^{inf} or \mathbb{Z}^{sup} . It is based on the set properties of \mathbb{Z}^{inf} and \mathbb{Z}^{sup} when $[\mathbf{m}]$ is split into several parts, i.e., $[\mathbf{m}] = \bigcup_i [\mathbf{m}_i]$. Indeed, we have

$$\begin{cases} \mathbb{Z}^{\text{sup}} = \text{proj}_X A \cap (X \times \bigcup_i [\mathbf{m}_i]) = \bigcup_i \text{proj}_X A \cap (X \times [\mathbf{m}_i]) = \bigcup_i \mathbb{Z}_i^{\text{sup}}, \\ \mathbb{Z}^{\text{inf}} = \overline{\text{proj}_X \bar{A} \cap (X \times \bigcup_i [\mathbf{m}_i])} = \bigcup_i \overline{\text{proj}_X \bar{A} \cap (X \times [\mathbf{m}_i])} = \bigcap_i \overline{\text{proj}_X \bar{A} \cap (X \times [\mathbf{m}_i])} = \bigcap_i \mathbb{Z}_i^{\text{inf}}. \end{cases} \quad (13)$$

Fig. 7 shows how \mathbb{Z}^{inf} and \mathbb{Z}^{sup} are obtained when $[\mathbf{m}]$ is split into two parts, i.e., $[\mathbf{m}] = [m_1] \cup [m_2] = [-10, 2] \cup [2, 10]$.

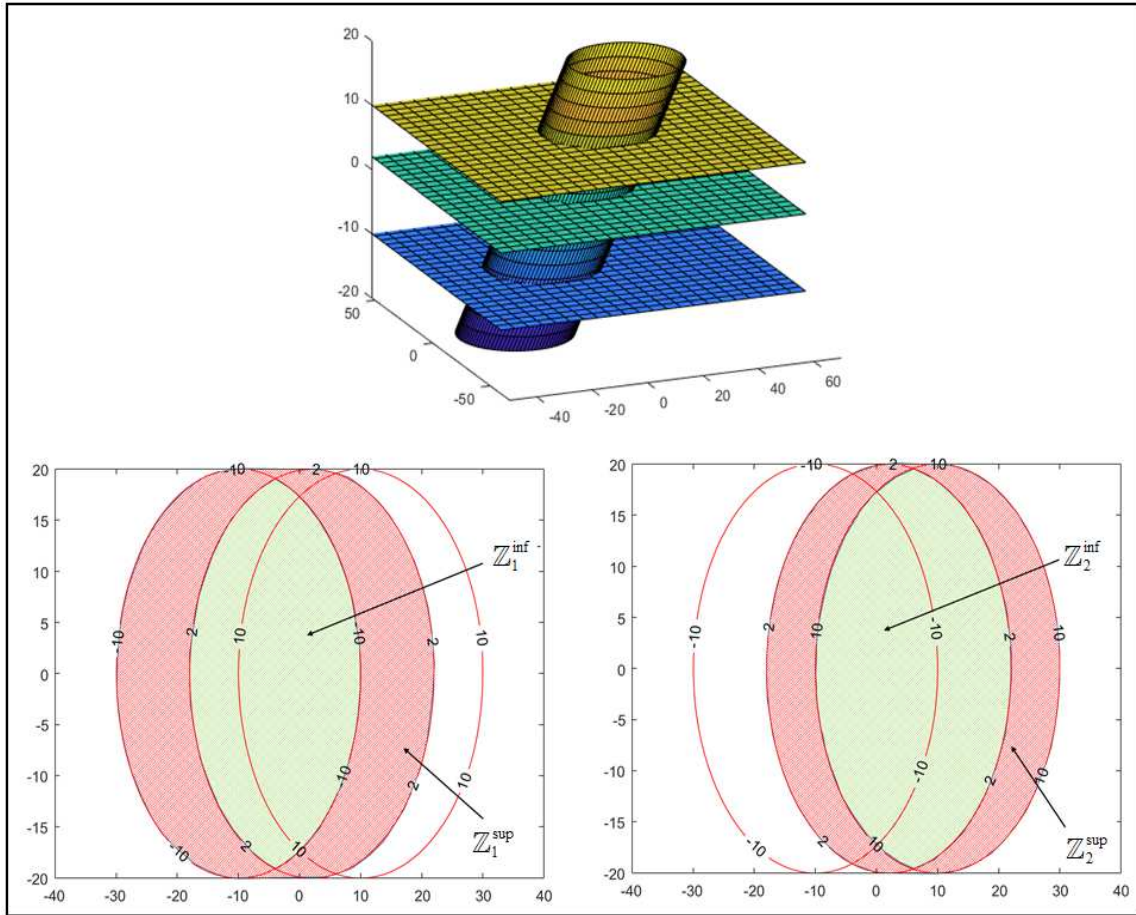


Fig. 7. Projection illustration for computing \mathbb{Z}^{inf} and \mathbb{Z}^{sup} .

We must note that \mathbb{Z}^{inf} , which is shown in Fig. 6(b), is the intersection of $\mathbb{Z}_1^{\text{inf}}$ and $\mathbb{Z}_2^{\text{inf}}$ shown in Fig. 7 because $\mathbb{Z}^{\text{inf}} = \mathbb{Z}_1^{\text{inf}} \cap \mathbb{Z}_2^{\text{inf}}$ according to (13). In the same manner, \mathbb{Z}^{sup} , which is shown in Fig. 6(b), is the union of $\mathbb{Z}_1^{\text{sup}}$ and $\mathbb{Z}_2^{\text{sup}}$ because $\mathbb{Z}^{\text{sup}} = \mathbb{Z}_1^{\text{sup}} \cup \mathbb{Z}_2^{\text{sup}}$. This principle can be generalized for the paving of $X \times [\mathbf{m}]$ by a set of boxes, i.e.,

$$X \times [\mathbf{m}] = \bigcup_{i,j} [x_i] \times [m_j]. \quad (14)$$

The paving algorithm proposed in [14] leads to efficient computations using the interval-based solver PyIbex (<https://www.ensta-bretagne.fr/desrochers/pyibex/docs/pyibex/>). PyIbex is a set of Python modules for solving nonlinear problems using interval-arithmetic tools. For practical implementation of the PyIbex interval-based solver, (13) is transformed into equations using logical quantifiers. Thus, we obtain

$$\begin{cases} \mathbf{Z}^{\text{sup}} = \{x \mid \exists m \in [m], \|x - m\| \leq 20\} = \text{proj}_x \{(x, m) \mid \|x - m\| \leq 20\}, \\ \mathbf{Z}^{\text{inf}} = \{x \mid \forall m \in [m], \|x - m\| \leq 20\} = \overline{\{x \mid \exists m \in [m], \|x - m\| > 20\}}, \\ = \overline{\text{proj}_x \{(x, m) \mid \|x - m\| > 20\}}. \end{cases} \quad (15)$$

CS \mathbf{Z}^{sup} is a plausible zone and is associated with existential quantifier \exists , whereas CS \mathbf{Z}^{inf} is a certain zone and is associated with universal quantifier \forall .

Fig. 7 shows the solution provided by the solver and represented by the visualization system VIBes (<http://codac.io/manual/07-graphics/01-vibes.html>) Communication zones \mathbf{Z}^{inf} and \mathbf{Z}^{sup} when $m_1 = [-10, 10]$ and $m_2 = [0, 0] = 0$ (i.e., $[m] = [-10, 10] \times [0, 0]$) are shown in Fig. 8 with and without a paving illustration. In the following study and for reasons of visibility, paving is often not shown in the figures. Equation (12) in \square^3 is used for ease in explanation and representation. Nevertheless, the principle is general and can be applied to the initial constraint in \square^4 , as expressed by (9), i.e., when (m_1, m_2) belongs to 2D box $[m]$. The results obtained for $[m] = [-1, 3] \times [1, 5]$ are shown in Fig. 9.

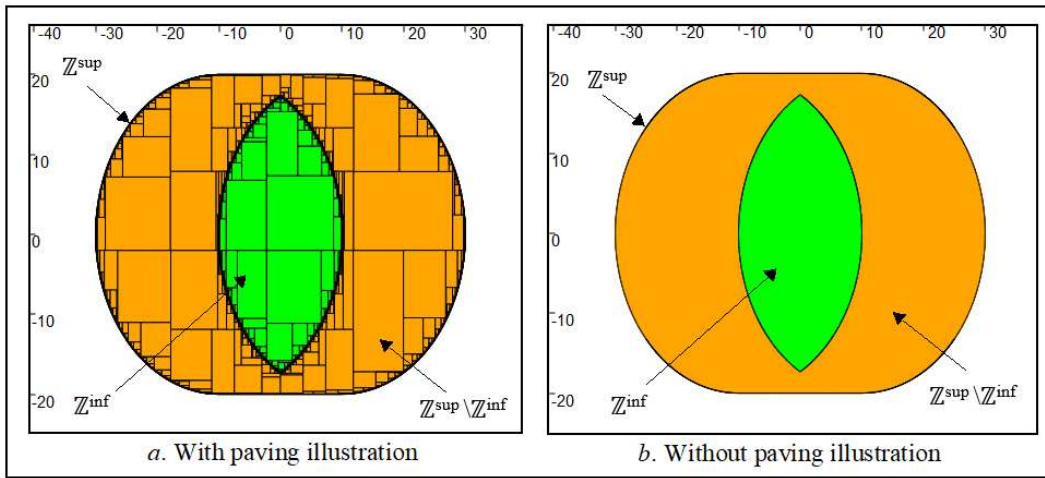


Fig. 8. Results of \mathbf{Z}^{inf} and \mathbf{Z}^{sup} using PyIbex for $[m] = [-10, 10] \times [0, 0]$.

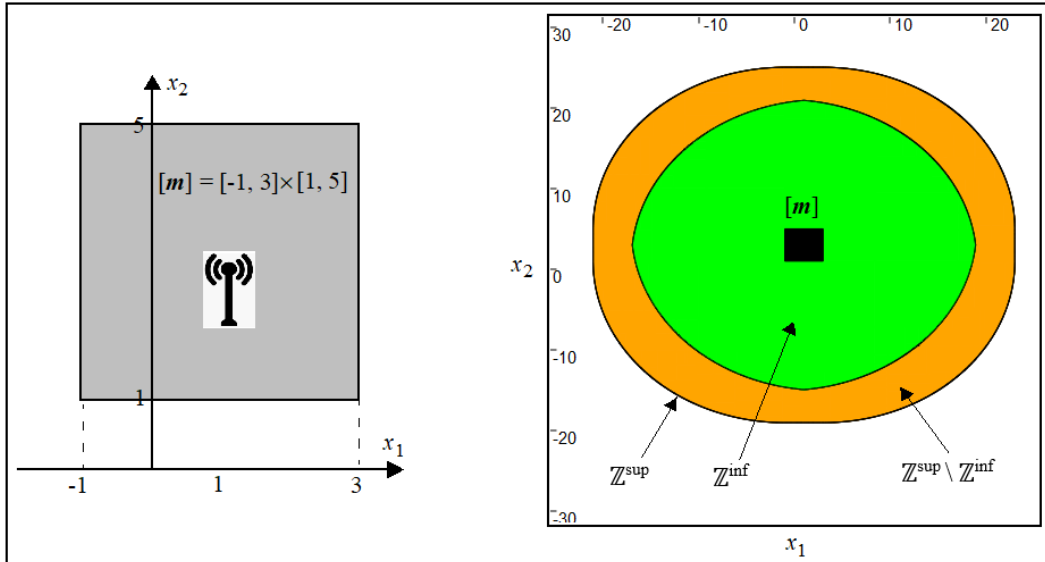


Fig. 9. Uncertain communication zone illustration for $[m] = [-1, 3] \times [1, 5]$.

2.4 GSs, TIFSs, and gradual boxes (GBs)

2.4.1 Definitions

Let L be a complete distributive lattice with top “1” and bottom “0.” In this study, L is considered as totally ordered and is taken as a unit interval. As discussed in [20], the elements of L can be

regarded as membership degrees for fuzzy sets and degrees of pertinence or of flexibility, among others. Let X be a CS. A GS G of X is defined using an assignment function A_G from $(0, 1]$ to 2^X , i.e.,

$$\forall \lambda \in (0,1]: A_G(\lambda) = X(\lambda). \quad (16)$$

In this study, the domain of λ is extended to $[0, 1]$, i.e., $X(0)$ is defined. Equation (16) indicates that the assignment function assigns to each degree λ a CS $X(\lambda)$ of \square^n . Therefore, the arithmetical and logical operators initially defined in CSs can naturally be extended to GSs. Furthermore, at each degree λ , the characteristic function of $X(\lambda)$, i.e., $\mu_{X(\lambda)}: \square^n \rightarrow \{0,1\}$, for all $\lambda \in [0, 1]$, is defined by

$$\mu_{X(\lambda)}(x) = \begin{cases} 1 & \text{if } x \in X(\lambda), \\ 0 & \text{if } x \notin X(\lambda). \end{cases} \quad (17)$$

Equation (17) is simply an extension of (2) with a gradual case where a vertical dimension λ is added to represent the gradual inclusion. In a gradual framework, the images of the assignment function are not necessarily nested [20]. Therefore, a GS is regarded as a stack of CSs that are not necessarily nested. Furthermore, the monotonicity (consistency) condition

$$\forall \lambda_1, \lambda_2 \in [0,1], \lambda_1 \leq \lambda_2 \Rightarrow X(\lambda_2) \subseteq X(\lambda_1), \quad (18)$$

which is required for TIFSs, is relaxed (not imposed) for GSs. Three examples of 2D GSs with their assignment functions $X_1(\lambda)$, $X_2(\lambda)$, and $X_3(\lambda)$ are shown in Fig. 10.

In the remainder of this paper, for simplicity of notation and when no confusion occurs, a GS is directly denoted by its assignment function $X(\lambda)$, $\lambda \in [0, 1]$. Furthermore, a CS is considered a special case of a GS with a constant assignment function.

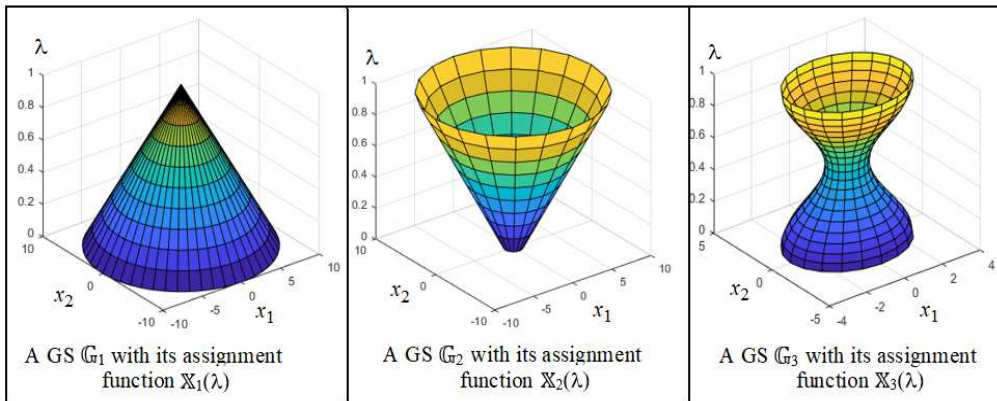


Fig. 10. Three 2D GSs.

Because a box is a particular case of a CS, a GB is a particular case of a GS. For instance, a 2D GB is shown in Fig. 11 with its assignment function $X(\lambda)$, i.e., at each level λ , $X(\lambda)$ is a box.

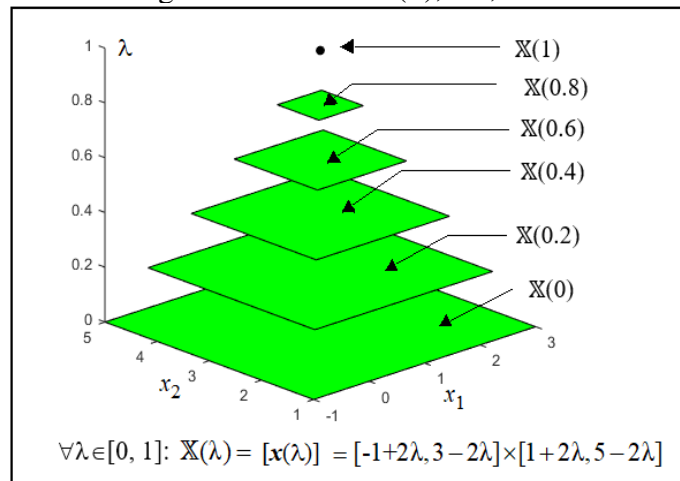


Fig. 11. 2D GB (a discrete representation with a sampling step of 0.2 on λ).

For reasons of homogeneity with the box notation, GBs can be represented by the well-known bracket notation. In this case, GB, with its assignment function $X(\lambda)$, can be denoted by $[x(\lambda)]$ (x in bold). Notation $[x(\lambda)]$ can be regarded as an assignment function that assigns a box for any degree λ . More generally, GB $[x(\lambda)]$, $\lambda \in [0, 1]$ is defined as

$$[x(\lambda)] = [x_1(\lambda)] \times [x_2(\lambda)] \times \dots \times [x_n(\lambda)], \text{ where } [x_i(\lambda)] = [x_i^-(\lambda), x_i^+(\lambda)] \text{ for } i = 1, \dots, n. \quad (19)$$

By comparing (19) and (4), we can confirm that a GB is simply a box parameterized by λ . Furthermore, a one-dimensional (1D) GB is a gradual interval (GI) that is represented by $[x(\lambda)] = [x^-(\lambda), x^+(\lambda)]$ [7][27].

2.4.2. GSs and TIFSs

A TIFS can be represented either by a membership function or by a family of nested CSs, which is called λ -level sets (λ -cuts). According to the representation theorem [53][58], any TIFS, which is denoted by \hat{X} , can be decomposed into a family $\{X(\lambda)\}_\lambda$, $\lambda \in [0, 1]$ of its λ -cuts under the constraint of monotonicity, i.e., (18). Hence, a λ -cut on a TIFS is CS $X(\lambda)$, $\lambda \in [0, 1]$, and the membership function of TIFS \hat{X} is obtained from the characteristic function of CSs by

$$\mu_{\hat{X}}(x) = \sup_{\lambda \in [0, 1]} \lambda \mu_{X(\lambda)}(x), \forall x \in \square^n. \quad (20)$$

When the consistency condition, i.e., (18), is guaranteed, a GS becomes a TIFS, where the assignment-function concept in GSs is substituted by the λ -cut principle in TIFSs. In this case, the membership function of a TIFS can be deduced from that of a GS using the assignment function and vice versa [20]. If a TIFS is a particular case of a GS, the reciprocal is false insofar as no monotony constraint is associated with the GS. For the others, a GS, where the consistency condition is followed, is called a consonant GS (or a TIFS). A non-consonant GS, which cannot be represented by a TIFS, is called a pure GS.

An interval-valued TIFS (IV-TIFS), also called a fuzzy interval or an interval-valued fuzzy number [22][27][67], is a particular case (1D representation) of a TIFS and can be regarded as a consonant GI [7][8]. For compatibility reasons with the interval notation, an IV-TIFS is often denoted by its λ -cuts $[x(\lambda)]$, $\lambda \in [0, 1]$. Each λ -cut is CI $[x(\lambda)] = [x^-(\lambda), x^+(\lambda)]$.

An IV-TIFS vector is defined by the Cartesian product of n IV-TIFSs. In this study, an IV-TIFS vector is called a box-valued TIFS (BV-TIFS) and is defined by its λ -cut representation, namely, (19), under the consistency constraint, i.e., a BV-TIFS is a consonant GB.

2.4.3 Illustration

The position of the transmitter remains uncertain but is now instantiated in boxes with the associated degrees of confidence. Thus, representing uncertain information, e.g., a transmitter is located in $[m]$ with a confidence of 50%, is made possible. These confidence levels may depend on the weather and some environmental factors. As mentioned in [7], [20], and [27], the idea of moving from a Boolean to a gradual context through a degree, which takes its values in the interval $[0, 1]$, makes illustrating the notion of progressive uncertainty possible. Therefore, the notion of progressivity in belonging to box $[m]$ enriches its representativeness and improves its specificity. The uncertain transmitter position can be represented by 2D GB $[m(\lambda)]$, $\lambda \in [0, 1]$, which can be interpreted as a 2D distribution of possibility. At each level λ , the transmitter is located in box $[m(\lambda)]$, and the communication zone is a TS. Fig. 12 shows gradual box $[m(\lambda)] = [-1+2\lambda, 3-2\lambda] \times [1+2\lambda, 5-2\lambda]$ for $\lambda = 0, 0.5$, and 1.

Therefore, box $[m(0)] = [-1, 3] \times [1, 5]$ corresponds to the most uncertain location of m , and $[m(1)] = [1, 1] \times [3, 3] = (1, 3)$ refers to its most precise (crisp) position.

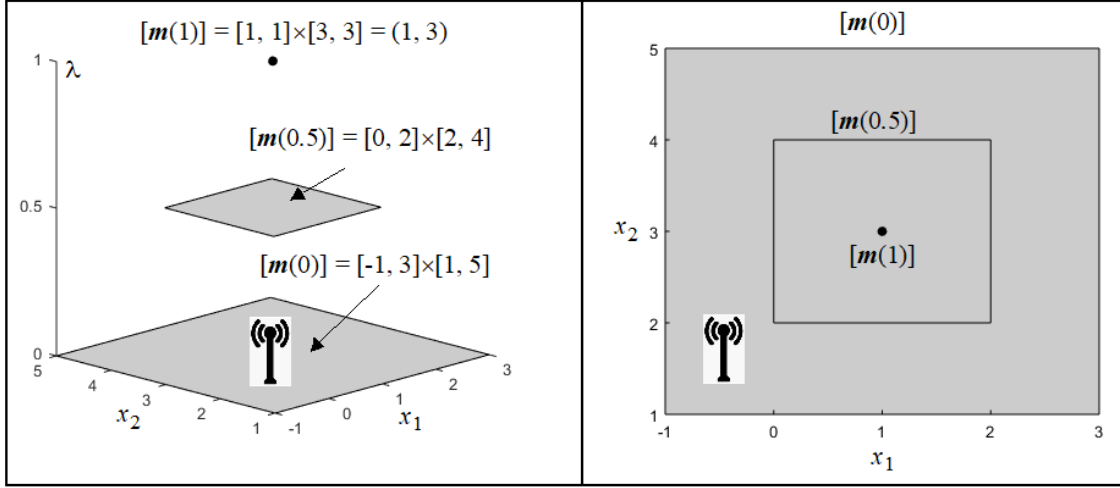


Fig. 12. Discrete representation of GB $[m(\lambda)]$ for $\lambda = 0, 0.5,$ and $1.$

2.5 TGSs, T2FSs, and thick GBs (TGBs)

2.5.1 Definitions

In an uncertain environment, because the concept of CSs has been extended to GSs, the concept of TSs can also be extended to TGSs. Therefore, a TGS, which is described by its assignment function $[[X(\lambda)]]$, can be defined as an interval of two GSs, namely, lower GS $X^{\text{inf}}(\lambda)$ and upper GSs $X^{\text{sup}}(\lambda)$, such that

$$[[X(\lambda)]] = [X^{\text{inf}}(\lambda), X^{\text{sup}}(\lambda)] = \{X(\lambda) \in P(\square^n) \mid X^{\text{inf}}(\lambda) \subset X(\lambda) \subset X^{\text{sup}}(\lambda)\}, \forall \lambda \in [0, 1]. \quad (21)$$

For each level $\lambda \in [0, 1]$, $[[X(\lambda)]]$ is a TS. In this case, the characteristic function of $[[X(\lambda)]]$, namely, $\mu_{[[X(\lambda)]]}: \square^n \rightarrow \{0, ?, 1\}$, for all $\lambda \in [0, 1]$, is expressed as

$$\mu_{[[X(\lambda)]]}(x) = \begin{cases} 1, & \text{if } x \in X^{\text{inf}}(\lambda), \\ 0, & \text{if } x \notin X^{\text{sup}}(\lambda), \\ ?, & \text{otherwise.} \end{cases} \quad (22)$$

Equations (21) and (22) are extensions of (5) and (6) to the gradual case, respectively, where all CSs are replaced by GSs, which are parameterized by λ .

By analogy to a GB, a TGB can be envisioned and regarded as a particular case of a TGS. For example, TGB $[[X(\lambda)]]$, $\lambda \in [0, 1]$, is shown in Fig. 13.

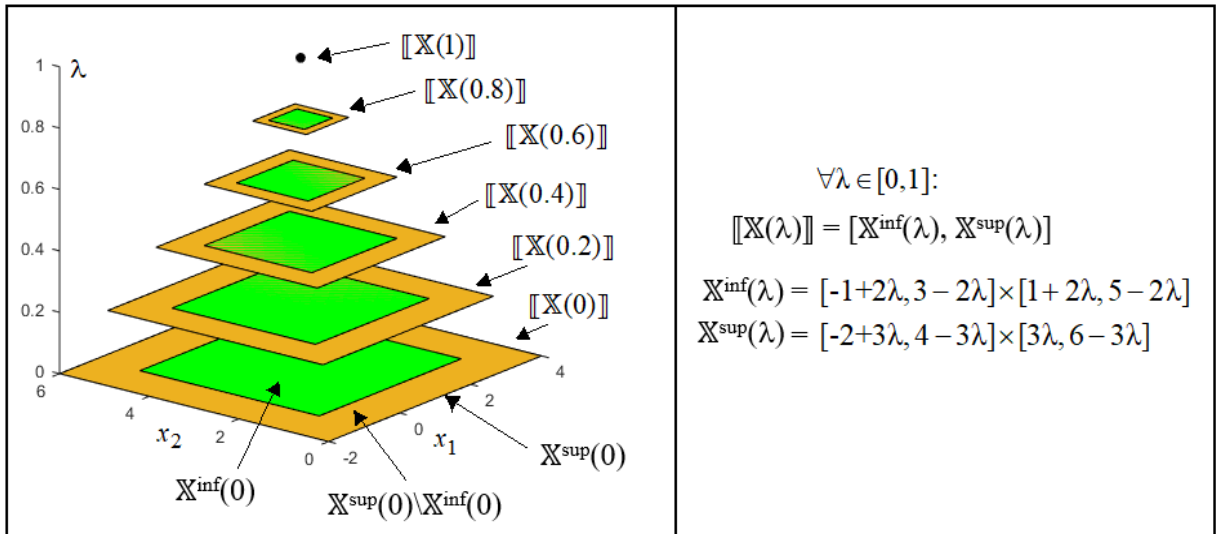


Fig. 13. Discrete representation of 2D TGS (TGB) with a sampling step of 0.2 on λ .

We can observe that at each level λ , $\llbracket \mathbb{X}(\lambda) \rrbracket$ is a TB. Furthermore, a thick GI (TGI) [6] is a 1D TGB. Another view (based on left and right GIs) that is specific to TGIs in the interval-arithmetic context has been proposed [6]. Here, TGIs are considered as GSs and are treated via a set-membership formalism. Even if the two representations are different, they lead to the same results.

In the TGS formalism, no monotonic constraint is imposed for GSs $\mathbb{X}^{\text{inf}}(\lambda)$ and $\mathbb{X}^{\text{sup}}(\lambda)$. In all circumstances, if $\mathbb{X}^{\text{inf}}(\lambda) = \mathbb{X}^{\text{sup}}(\lambda)$, TGS $\llbracket \mathbb{X}(\lambda) \rrbracket$ becomes GS $\mathbb{X}(\lambda)$.

2.5.2 TGSs and T2FSs

In the TGS representation, if GS bounds $\mathbb{X}^{\text{inf}}(\lambda)$ and $\mathbb{X}^{\text{sup}}(\lambda)$ are consonant, i.e., they are represented by T1FSs. Then, a TGS becomes a TFS. Therefore, a TFS can be defined by a system (a family) of nested TSs $\{\llbracket \mathbb{X}(\lambda) \rrbracket\}_{\lambda; \lambda \in [0,1]}$ of its λ -cuts under the following monotonicity constraint:

$$\lambda_1 \leq \lambda_2 \Rightarrow \llbracket \mathbb{X}(\lambda_2) \rrbracket \subseteq \llbracket \mathbb{X}(\lambda_1) \rrbracket \Leftrightarrow \lambda_1 \leq \lambda_2 \Rightarrow \mathbb{X}^{\text{inf}}(\lambda_2) \subseteq \mathbb{X}^{\text{inf}}(\lambda_1) \text{ and } \mathbb{X}^{\text{sup}}(\lambda_2) \subseteq \mathbb{X}^{\text{sup}}(\lambda_1). \quad (23)$$

Therefore, TFS $\llbracket \hat{\mathbb{X}} \rrbracket$, which is considered as a family of λ -cuts, has its thick membership function defined by

$$\mu_{\llbracket \hat{\mathbb{X}} \rrbracket}(x) = \sup_{\lambda \in [0,1]} \lambda \mu_{\llbracket \hat{\mathbb{X}}(\lambda) \rrbracket}(x) = \llbracket \sup_{\lambda \in [0,1]} \lambda \mu_{\mathbb{X}^{\text{inf}}(\lambda)}(x), \sup_{\lambda \in [0,1]} \lambda \mu_{\mathbb{X}^{\text{sup}}(\lambda)}(x) \rrbracket, \forall x \in \mathbb{R}^n. \quad (24)$$

From (24), we can state that a TFS is represented by an interval of T1FSs. In cases when $\mathbb{X}^{\text{inf}}(\lambda) = \mathbb{X}^{\text{sup}}(\lambda) = \mathbb{X}(\lambda)$, TFS becomes a T1FS. Furthermore, because TFS is composed of two T1FSs (lower and upper T1FSs) under constraint $\mathbb{X}^{\text{inf}}(\lambda) \subseteq \mathbb{X}^{\text{sup}}(\lambda)$, $\forall \lambda \in [0,1]$, this condition implies that a TFS can be regarded as a special case of a T2FS. The lower bound represents a T1FS, which is certain. The T1FS upper bound delimits all plausible T1FSs. The uncertainty is exhibited by penumbra $\mathbb{X}^{\text{sup}}(\lambda) \setminus \mathbb{X}^{\text{inf}}(\lambda)$, $\forall \lambda \in [0,1]$. This penumbra concept in the TFS representation can be regarded as the FOU phenomenon in the T2FS representation [46][51].

A thick IV-T1FS (TIV-T1FS) $\llbracket \hat{x} \rrbracket$ is a special case of a TFS, i.e., a 1D TFS, and is represented by its membership function

$$\mu_{\llbracket \hat{x} \rrbracket}(x) = \llbracket \sup_{\lambda \in [0,1]} \lambda \mu_{\llbracket x^{\text{inf}}(\lambda) \rrbracket}(x), \sup_{\lambda \in [0,1]} \lambda \mu_{\llbracket x^{\text{sup}}(\lambda) \rrbracket}(x) \rrbracket, \forall x \in \mathbb{R}. \quad (25)$$

Therefore, a TIV-T1FS is an interval with lower and upper IV-T1FSs. A TIV-T1FS vector is called a thick BV-T1FS (TBV-T1FS) and is defined by the Cartesian product of n TIV-T1FS. We need to note that a TIV-T1FS is a particular case of a TGB and can be interpreted as an interval-valued T2FS (IV-T2FS) [24][26][30][59][69].

2.5.3 Illustration

The transmitter location is now represented by GB $\llbracket m(\lambda) \rrbracket$. The communication zone becomes a TGS $\llbracket \mathbb{Z}(\lambda) \rrbracket$, $\lambda \in [0, 1]$, which is shown in Figs. 14 and 15 for three chosen values of λ (0, 0.5, and 1). Nevertheless, the proposed computational method applies irrespective of the value of λ in $[0, 1]$.

The colors in Fig. 15 are only used to differentiate the λ levels. The case of $\lambda = 0$ corresponds to the situation presented in Section 2.3.2, and for each λ level, the communication zone is computed using the same methodology. Furthermore, the case of $\lambda = 1$ refers to the situation presented in Section 2.1 where the location of the transmitter is crisp and known with certainty. According to these results, we can confirm that if the location of the transmitter is uncertain, the communication zone is a TS. However, if its location is crisp, the communication zone is a CS (see Fig. 14), i.e., $\mathbb{Z}^{\text{sup}}(1) = \mathbb{Z}^{\text{inf}}(1) = \mathbb{Z}(1)$. In this application, we can confirm that $\mathbb{Z}^{\text{sup}}(1) \subseteq \mathbb{Z}^{\text{sup}}(0.5) \subseteq \mathbb{Z}^{\text{sup}}(0)$ [see Fig. 15(a)]. More generally, we can verify that the monotonicity (consistency) condition, i.e., (18), is observed for $\mathbb{Z}^{\text{sup}}(\lambda)$. In this case, upper bound $\mathbb{Z}^{\text{sup}}(\lambda)$ can be regarded as a T1FS. This situation of monotonicity (consistency) is a special case of the GS representation. More generally, no constraint of monotonicity is imposed on the GS and TGS representations. In contrast to $\mathbb{Z}^{\text{sup}}(\lambda)$, GS $\mathbb{Z}^{\text{inf}}(\lambda)$ does not obey constraint (18), i.e., $\mathbb{Z}^{\text{inf}}(1) \not\subseteq \mathbb{Z}^{\text{inf}}(0.5) \not\subseteq \mathbb{Z}^{\text{inf}}(0)$. In reality, we rather have the opposite

condition, i.e., $\mathbb{Z}^{\text{inf}}(0) \subset \mathbb{Z}^{\text{inf}}(0.5) \subset \mathbb{Z}^{\text{inf}}(1)$ [see Fig. 15(b)]. Therefore, $\mathbb{Z}^{\text{inf}}(\lambda)$ is a pure GS and cannot be represented by a T1FS. Thus, $[[\mathbb{Z}(\lambda)]]$, $\lambda \in [0, 1]$, is a TGS and cannot be interpreted as a T2FS.

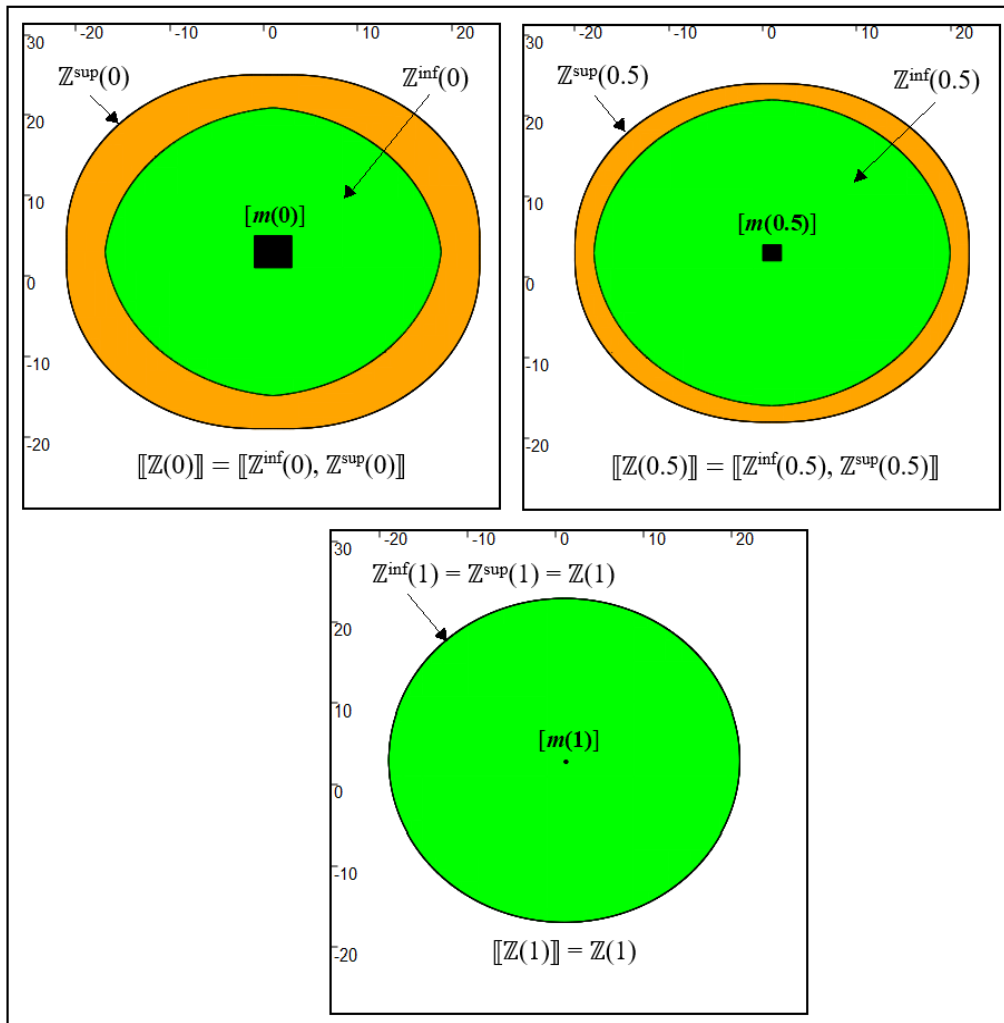


Fig. 14. Communication zone $[[\mathbb{Z}(\lambda)]]$ for $\lambda = 0, 0.5, 1$.

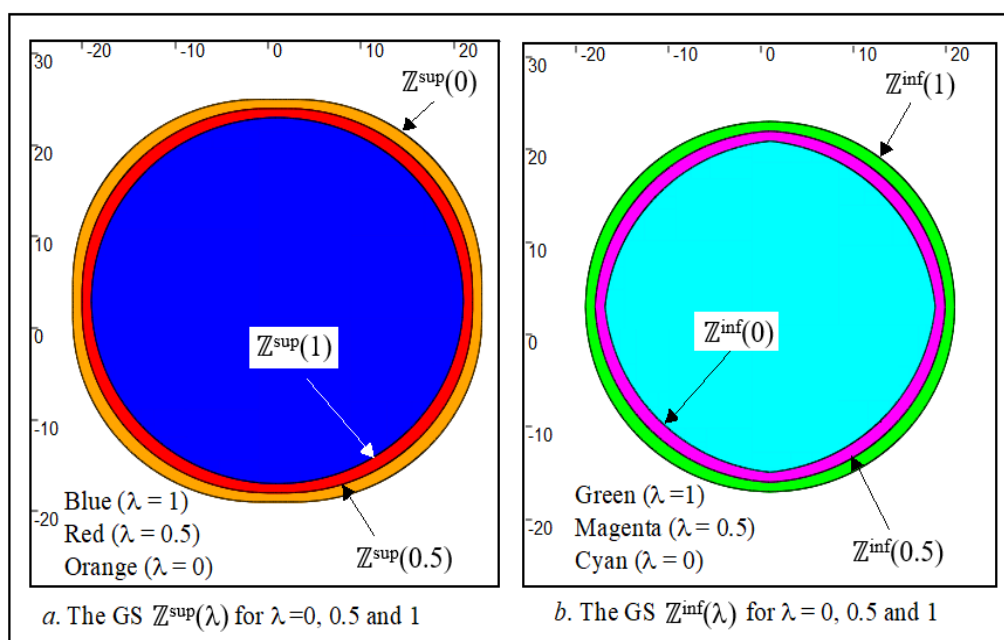


Fig. 15. GSs $Z^{\text{inf}}(\lambda)$ and $Z^{\text{sup}}(\lambda)$ for $\lambda = 0, 0.5, 1$.

2.6 Combination and fusion of TGSs

2.6.1 Definitions

Let us consider a collection of CSs $\{\mathbb{X}_i\}_{i \in \Omega}$. Smallest TS, which is denoted by $\&\{\mathbb{X}_i\}_{i \in \Omega}$ that encloses collection $\{\mathbb{X}_i\}_{i \in \Omega}$, is defined by

$$\&\{\mathbb{X}_i\}_{i \in \Omega} = \left[\bigcap_{i \in \Omega} \mathbb{X}_i, \bigcup_{i \in \Omega} \mathbb{X}_i \right]. \quad (26)$$

The $\&$ operator makes possible extension of the operators initially proposed for CSs to TSs [18][19]. Indeed, given an operator $\bullet \in \{\cap, \cup, \setminus, \dots\}$, its extension to TS is expressed as

$$\left[\mathbb{X} \bullet \mathbb{Y} \right] = \&\{T \mid \exists X \in \mathbb{X}, \exists Y \in \mathbb{Y}, T = X \bullet Y\}. \quad (27)$$

Equation (27) states that the result of an operation among TSs is defined as smallest TS computed from the operands. Knowing that at each λ level, a TGS is a TS, the operations on TGSs can be computed as operations on TSs. For instance, according to the monotony property of the intersection, union, difference, and addition operators, we have

$$\begin{cases} \left[\mathbb{X}(\lambda) \cap \mathbb{Y}(\lambda) \right] = \left[\mathbb{X}^{\text{inf}}(\lambda) \cap \mathbb{Y}^{\text{inf}}(\lambda), \mathbb{X}^{\text{sup}}(\lambda) \cap \mathbb{Y}^{\text{sup}}(\lambda) \right] \\ \left[\mathbb{X}(\lambda) \cup \mathbb{Y}(\lambda) \right] = \left[\mathbb{X}^{\text{inf}}(\lambda) \cup \mathbb{Y}^{\text{inf}}(\lambda), \mathbb{X}^{\text{sup}}(\lambda) \cup \mathbb{Y}^{\text{sup}}(\lambda) \right] \\ \left[\mathbb{X}(\lambda) \setminus \mathbb{Y}(\lambda) \right] = \left[\mathbb{X}^{\text{inf}}(\lambda) \setminus \mathbb{Y}^{\text{sup}}(\lambda), \mathbb{X}^{\text{sup}}(\lambda) \setminus \mathbb{Y}^{\text{inf}}(\lambda) \right] \\ \left[\mathbb{X}(\lambda) + \mathbb{Y}(\lambda) \right] = \left[\mathbb{X}^{\text{inf}}(\lambda) + \mathbb{Y}^{\text{inf}}(\lambda), \mathbb{X}^{\text{sup}}(\lambda) + \mathbb{Y}^{\text{sup}}(\lambda) \right] \end{cases}. \quad (28)$$

These operations are simply operations among TSs that are parameterized by λ . More generally, for a given function f from \square^n to \square^m , the image of TS $\left[\mathbb{X}(\lambda) \right] = \left[\mathbb{X}^{\text{inf}}(\lambda), \mathbb{X}^{\text{sup}}(\lambda) \right]$ by f is evaluated by

$$f\left(\left[\mathbb{X}(\lambda) \right]\right) = \&\{f(X(\lambda)) \mid X(\lambda) \in \left[\mathbb{X}(\lambda) \right]\} = \left[f\left(\mathbb{X}^{\text{inf}}(\lambda)\right), f\left(\mathbb{X}^{\text{sup}}(\lambda)\right) \right]. \quad (29)$$

The image of a TS $\left[\mathbb{X}(\lambda) \right]$ by f is also a TS in which its bounds are the images by f of the bounds of $\left[\mathbb{X}(\lambda) \right]$. This extension of functions allows the propagation of TSs and TGSs in linear and nonlinear models where the inputs, outputs, states, and/or parameters can be represented by TGSs.

2.6.2 Illustration

Let us reconsider the application of an autonomous vehicle and assume that three uncertain transmitters exist. The location of these transmitters is given by 2D GBs

$$\begin{cases} [m_1(\lambda)] = [-1+2\lambda, 3-2\lambda] \times [1+2\lambda, 5-2\lambda], \\ [m_2(\lambda)] = [11-3\lambda, 16-8\lambda] \times [-15+6\lambda, -5-4\lambda], \\ [m_3(\lambda)] = [8+2\lambda, 12-2\lambda] \times [-3+2\lambda, 1-2\lambda]. \end{cases} \quad (30)$$

We need to note that the proposed method can be applied regardless of the number of transmitters and their locations. Gradual zones $\mathbb{Z}^{\text{inf}}(\lambda)$ and $\mathbb{Z}^{\text{sup}}(\lambda)$ are computed as

$$\begin{cases} \mathbb{Z}^{\text{sup}}(\lambda) = \{x \mid \forall i \in \{1, \dots, 3\}, \exists m \in [m_i(\lambda)], \|x - m\| \leq 20\} \\ \quad = \bigcap_{i \in \{1, \dots, 3\}} \{x \mid \exists m \in [m_i(\lambda)], \|x - m\| \leq 20\}, \\ \mathbb{Z}^{\text{inf}}(\lambda) = \{x \mid \forall i \in \{1, \dots, 3\}, \forall m \in [m_i(\lambda)], \|x - m\| \leq 20\} \\ \quad = \bigcap_{i \in \{1, \dots, 3\}} \{x \mid \forall m \in [m_i(\lambda)], \|x - m\| \leq 20\} \\ \quad = \bigcap_{i \in \{1, \dots, 3\}} \overline{\{x \mid \exists m \in [m_i(\lambda)], \|x - m\| > 20\}}. \end{cases} \quad (31)$$

Equation (31) is simply a version of (15) in the presence of three transmitters instead of one. Thus, the communication zone is the intersection among the three zones where each one is obtained for a transmitter. TSs that represents the uncertain communication zone for $\lambda = 0, 0.5$, and 1 is shown in Fig. 16.

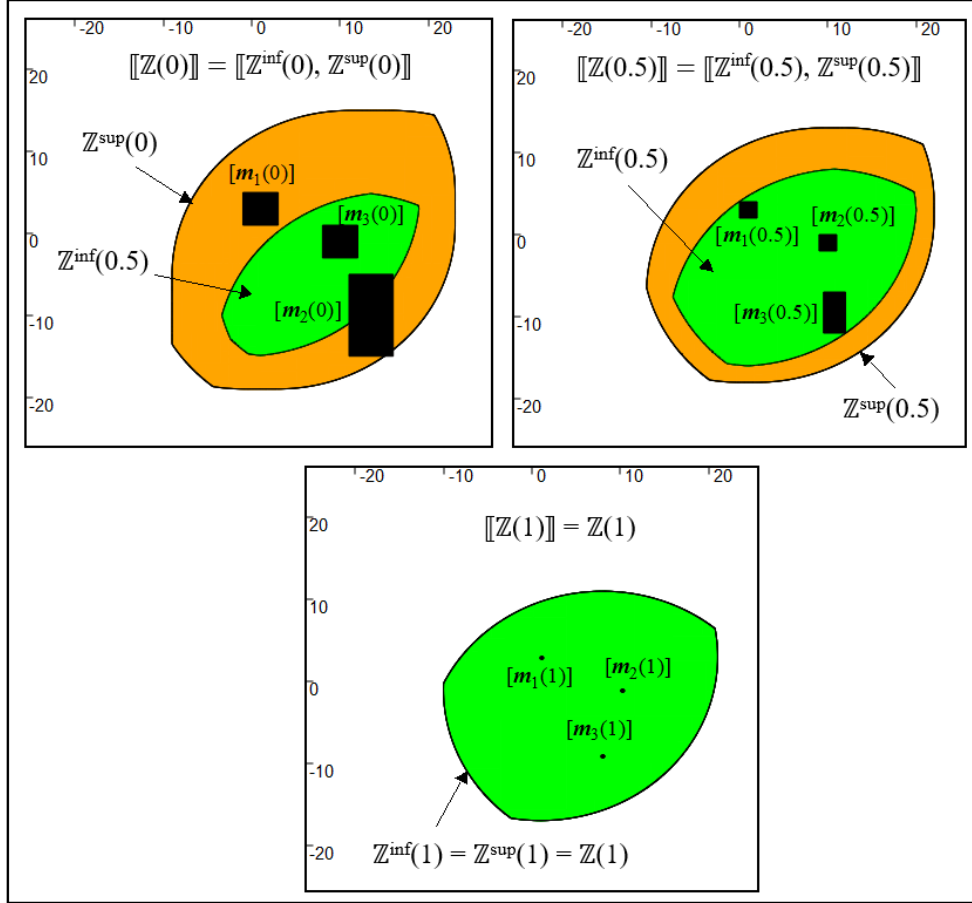


Fig. 16. Communication zone $\llbracket Z(\lambda) \rrbracket$ for $\lambda = 0, 0.5$, and 1 (using three transmitters).

The superposition of CSs $Z^{\text{inf}}(\lambda)$ and $Z^{\text{sup}}(\lambda)$ (each of them separately considered) leads to that shown Fig. 17. We need to note that the method applies regardless of the value of λ . Fig. 17 shows that $Z^{\text{inf}}(\lambda)$ and $Z^{\text{sup}}(\lambda)$ are pure GSs (no monotonicity constraint is imposed). Consequently, communication zone $\llbracket Z(\lambda) \rrbracket$ is a TGS.

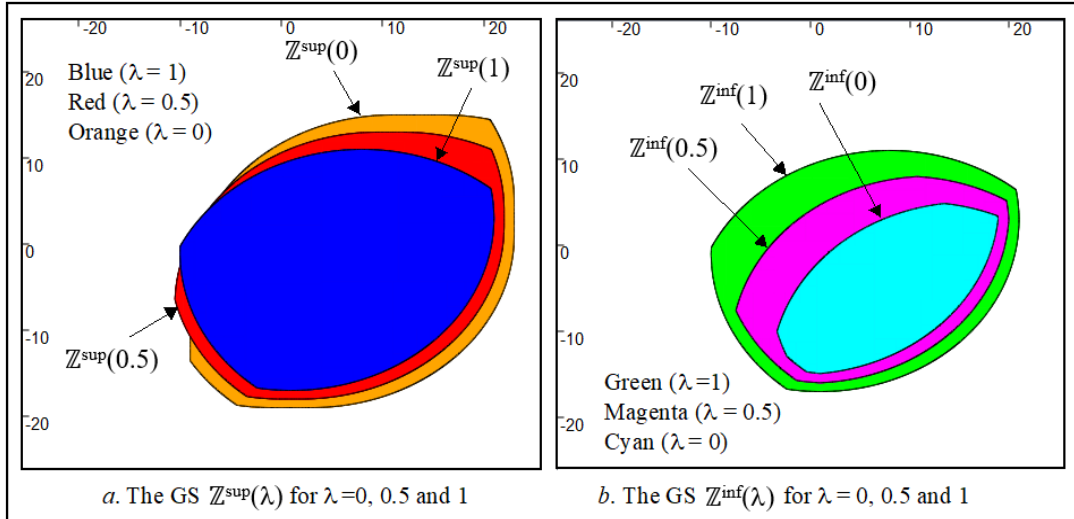


Fig. 17. Zones $Z^{\text{inf}}(\lambda)$ and $Z^{\text{sup}}(\lambda)$ for $\lambda = 0, 0.5$, and 1 (using three transmitters).

As presented in Section 2.5.3, at each level λ , the uncertain location of the transmitters induces a TS. The uncertainty (ignorance) is exhibited by penumbra $Z^{\text{sup}}(\lambda) \setminus Z^{\text{inf}}(\lambda)$, which is shown in orange colors in Fig. 16. In contrast, when the transmitters are located with precision, i.e., $\lambda = 1$, the communication zone is a CS, where $Z^{\text{inf}}(\lambda) = Z^{\text{sup}}(\lambda)$.

3 Applications of TGSs

In this section, applications for solving fuzzy SoEs and fuzzy regression are provided to illustrate the usefulness and interest of the TGS concept. Many other applications of the TGS approach can be envisioned in uncertain control and modeling and uncertain optimization, among others.

3.1 Solving fuzzy SoEs

For the sake of simplicity, linear fuzzy SoEs are considered. However, the method can be applied in whatever equation forms. Furthermore, for ease in three-dimensional (3D) illustration, only SoEs with two variables are considered. However, the method remains applicable regardless of the number of variables.

Solving linear SoEs $A \times \mathbf{x} = \mathbf{b}$ where the parameters of matrix $A(n \times n)$ and vector $\mathbf{b}(1 \times n)$ are crisp values has a very long history. This problem has been extended to the fuzzy case where the parameters are often represented by IV-T1FSs [2][28][38][40]. For example, linear SoEs whose parameters are IV-T1FS are often denoted by its λ -cut representation, i.e.,

$$[A(\lambda)] \times \mathbf{x} = [\mathbf{b}(\lambda)], \forall \lambda \in [0, 1], \quad (32)$$

$$\text{where } [A(\lambda)] = \begin{pmatrix} [a_{11}(\lambda)] & \cdots & [a_{1n}(\lambda)] \\ \vdots & \ddots & \vdots \\ [a_{n1}(\lambda)] & \cdots & [a_{nn}(\lambda)] \end{pmatrix}, [\mathbf{b}(\lambda)] = \begin{pmatrix} [b_1(\lambda)] \\ \cdots \\ [b_n(\lambda)] \end{pmatrix} \text{ and } \mathbf{x} = \begin{pmatrix} x_1 \\ \cdots \\ x_n \end{pmatrix}.$$

Conceptually, fuzzy SoEs, i.e., (32), have often been approached as interval SoEs via the concept of λ -cuts [2][3][28]. Solving SoEs that involve CIs and IV-T1FSs has been investigated for quite a long time (e.g. [2], [3], [25], [28], [31], [56], [61], [63], and [66]). Although significant advances have been achieved in solving these fuzzy SoEs, two important considerations deserve special attention. The first consideration concerns the algebraic solution of (32). The second consideration is related to the meaning and significance associated with this solution, more particularly the united and tolerable solutions. These two considerations are addressed using the following two applications.

3.1.1 Example 1

Generally, the algebraic solution of (32) corresponds to the exact solution (sometimes called the formal solution) [2][25]. This solution is usually too restrictive and sometimes even fails to exist. Generally, embedded approaches according to the Kaucher interval arithmetic [35] are used to solve these SoEs [28][61]. Therefore, when they exist, the solutions are computed at each level λ . However, the resulting solutions can sometimes be non-nested according to the vertical λ dimension. In this case, although the parameters of (32) are IV-T1FSs, the resulting solutions can be purely gradual quantities and cannot be regarded as fuzzy quantities [2][8][27][40].

Let us consider the 2×2 fuzzy linear SoEs, which have been considered in [2], as a counter-example of the fuzzy approach proposed in [28] with the following parameters:

$$A = \begin{pmatrix} a_{11} & a_{12} \\ a_{21} & a_{22} \end{pmatrix} = \begin{pmatrix} 1 & -1 \\ 1 & 3 \end{pmatrix}, [\mathbf{b}(\lambda)] = \begin{pmatrix} [b_1(\lambda)] \\ [b_2(\lambda)] \end{pmatrix} \text{ and } \mathbf{x} = \begin{pmatrix} x_1 \\ x_2 \end{pmatrix}, \quad (33)$$

$$\text{where } \begin{cases} [b_1(\lambda)] = [b_1^-(\lambda), b_1^+(\lambda)] = \begin{cases} [8\lambda - 14, -1 - 13\lambda], & \text{if } 0 \leq \lambda \leq 0.5, \\ [2\lambda - 11, -6 - 3\lambda], & \text{if } 0.5 \leq \lambda \leq 1, \end{cases} \\ [b_2(\lambda)] = [b_2^-(\lambda), b_2^+(\lambda)] = \begin{cases} [12\lambda - 24, -18\lambda - 2], & \text{if } 0 \leq \lambda \leq 0.5, \\ [6\lambda - 21, -7 - 8\lambda], & \text{if } 0.5 \leq \lambda \leq 1. \end{cases} \end{cases}$$

In (33), the elements of A are crisp values, and those of $[\mathbf{b}(\lambda)]$ are triangular IV-T1FSs, which are represented by their λ -cuts. IV-T1FSs of $[\mathbf{b}(\lambda)]$ are shown in Figs. 18(a) and (b). At each λ -cut, these IV-T1FSs are considered as box $[\mathbf{b}(\lambda)] = [b_1(\lambda)] \times [b_2(\lambda)]$ in plane (b_1, b_2) . The stacking of boxes $[\mathbf{b}(\lambda)]$ according to λ leads to BV-T1FS shown in Fig. 18(c) using a sampling step size of 0.05 on λ , i.e.,

$$\sup_{\lambda \in [0,1]} \lambda \mu_{[b(\lambda)]}(\mathbf{x}), \forall \mathbf{x} \in \square^2; \text{ where } [b(\lambda)] = [b_1(\lambda)] \times [b_2(\lambda)]. \quad (34)$$

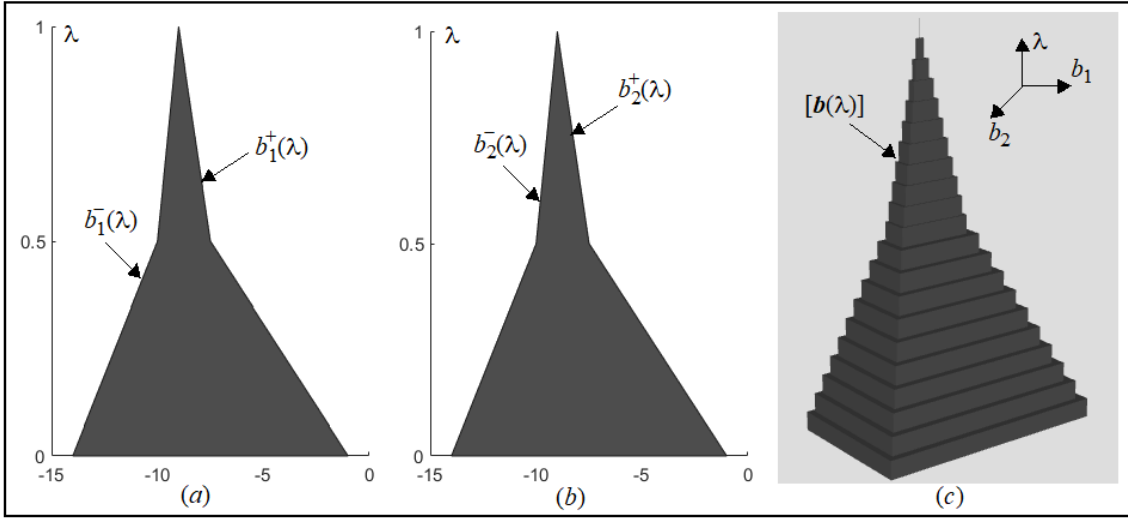


Fig. 18. Representations of IV-T1FSs $[b_1(\lambda)]$ and $[b_2(\lambda)]$ and BV-T1FS $[b(\lambda)]$.

The algebraic solution of the fuzzy SoEs, i.e., (33), which is addressed in [2], is expressed as

$$\begin{cases} [x_1(\lambda)] = [x_1^-(\lambda), x_1^+(\lambda)], \text{ with } x_1^-(\lambda) = \begin{cases} 4\lambda - 4, & \text{if } 0 \leq \lambda \leq 1/4, \\ -3, & \text{if } 1/4 \leq \lambda \leq 3/8, \\ -8\lambda, & \text{if } 3/8 \leq \lambda \leq 1/2, \\ 2\lambda - 5, & \text{if } 1/2 \leq \lambda \leq 1, \end{cases} ; x_1^+(\lambda) = \begin{cases} -8\lambda, & \text{if } 0 \leq \lambda \leq 1/3, \\ 4\lambda - 4, & \text{if } 1/3 \leq \lambda \leq 1/2, \\ -8\lambda - 1, & \text{if } 1/2 \leq \lambda \leq 1, \end{cases} \\ [x_2(\lambda)] = [x_2^-(\lambda), x_2^+(\lambda)] = [4\lambda - 10, -1 - 5\lambda]. \end{cases} \quad (35)$$

Solutions $[x_1(\lambda)]$ and $[x_2(\lambda)]$ are shown in Figs. 19(a) and (b), respectively. We can state that if $[x_2(\lambda)]$ is an IV-T1FS, $[x_1(\lambda)]$ is a pure GI and cannot be represented by an IV-T1FS. Therefore, profiles $x_2^-(\lambda)$ and $x_2^+(\lambda)$ are non-decreasing and non-increasing, respectively, i.e., the consistency condition, namely, (18), is not followed. Furthermore, at each level λ , solutions $[x_1(\lambda)]$ and $[x_2(\lambda)]$ can be represented by box $[x(\lambda)] = [x_1(\lambda)] \times [x_2(\lambda)]$ in plane (x_1, x_2) . Fig. 19(c) shows that when a sampling step size of 0.05 on λ is used, the stacking of boxes $[x(\lambda)]$ according to λ cannot be interpreted as a BV-T1FS but as a pure GB. Therefore, boxes $[x(\lambda)]$, $\lambda \in [0, 1]$ are not always nested according to the λ dimension, i.e., the monotonicity (consistency) condition, namely, (18), is not satisfied. Although the parameters of fuzzy SoEs, namely, (33), are IV-T1FS (a BV-T1FS), the solution is not a BV-T1FS and cannot be regarded as a fuzzy set.

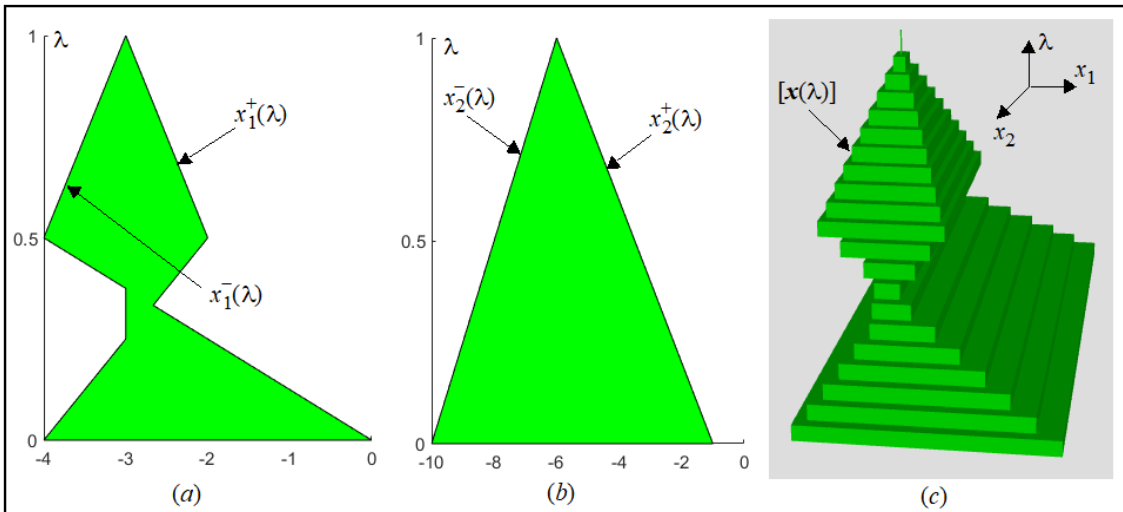


Fig. 19. Representation of the solutions of fuzzy SoEs (33).

In this case and as stated in [2], a fuzzy solution of (33) does not exist, and the solution proposed in [28] cannot be considered as a fuzzy solution. Therefore, we can state that the solution given in [2] is a GB, which is a particular case of a GS. In this context, the GB and GS concepts provide a new outlook for interpreting the solutions of fuzzy SoEs when the results are not fuzzy quantities.

Let us reconsider the SoEs, namely, (33), where the parameters of $[b(\lambda)]$ are no longer IV-T1FSs but IV-T2FSs. Each IV-T2FS $[\tilde{b}_i(\lambda)]$ is defined by two IV-T1FSs, namely, lower $[b_i^{\text{inf}}(\lambda)]$ and upper $[b_i^{\text{sup}}(\lambda)]$ IV-T1FSs, with inclusion constraint $[b_i^{\text{inf}}(\lambda)] \subseteq [b_i^{\text{sup}}(\lambda)]$ [5]. In this case, SoEs, i.e., (33), become

$$\begin{pmatrix} 1 & -1 \\ 1 & 3 \end{pmatrix} \times \mathbf{x} = \begin{pmatrix} [\tilde{b}_1(\lambda)] \\ [\tilde{b}_2(\lambda)] \end{pmatrix}, \forall \lambda \in [0,1], \text{ with } \mathbf{x} = \begin{pmatrix} x_1 \\ x_2 \end{pmatrix}; \quad \begin{cases} [b_1^{\text{inf}}(\lambda)] = [b_1(\lambda)], \\ [b_2^{\text{inf}}(\lambda)] = [b_2(\lambda)], \\ [b_1^{\text{sup}}(\lambda)] = \begin{cases} [10\lambda - 17, 2 - 16\lambda], & \text{if } 0 \leq \lambda \leq 0.5, \\ [6\lambda - 15, -3 - 6\lambda], & \text{if } 0.5 \leq \lambda \leq 1, \end{cases} \\ [b_2^{\text{sup}}(\lambda)] = \begin{cases} [16\lambda - 27, -22\lambda + 1], & \text{if } 0 \leq \lambda \leq 0.5, \\ [8\lambda - 23, -5 - 10\lambda], & \text{if } 0.5 \leq \lambda \leq 1. \end{cases} \end{cases} \quad (36)$$

IV-T2FS SoEs, i.e., (36), can be viewed as lower and upper IV-T1FS SoEs in the form of (33). IV-T2FSs are shown in Figs. 20(a) and (b). We can state that a λ -cut on each IV-T2FS is a TI, i.e.,

$$\square [b_i(\lambda)] \square = \square [b_i^{\text{inf}}(\lambda), [b_i^{\text{sup}}(\lambda)] \square, \quad i = 1, 2. \quad (37)$$

Therefore, each IV-T2FS can be interpreted as a TIV-T1FS, which is expressed as

$$\square \sup_{\lambda \in [0,1]} \lambda \mu_{[b_i^{\text{inf}}(\lambda)]}(\mathbf{x}), \sup_{\lambda \in [0,1]} \lambda \mu_{[b_i^{\text{sup}}(\lambda)]}(\mathbf{x}) \square, \quad i = 1, 2. \quad (38)$$

Furthermore, at each level λ , IV-T2FSs can be regarded as a TB in plane (b_1, b_2) , i.e.,

$$\square [b(\lambda)] \square = \square [b_1(\lambda)] \square \times \square [b_2(\lambda)] \square = \square [b^{\text{inf}}(\lambda), [b^{\text{sup}}(\lambda)] \square, \quad (39)$$

with $[b^{\text{inf}}(\lambda)] = [b_1^{\text{inf}}(\lambda)] \times [b_2^{\text{inf}}(\lambda)]$ and $[b^{\text{sup}}(\lambda)] = [b_1^{\text{sup}}(\lambda)] \times [b_2^{\text{sup}}(\lambda)]$.

The stacking of these TBs according to λ leads to TBV-T1FS, which is shown in Fig. 20(c), using a sampling step size of 0.05 on λ . By applying the approach proposed in [2], the lower and upper algebraic solutions of (36) are

$$\begin{cases} [x_1^{\text{inf}}(\lambda)] = [x_1(\lambda)], \\ [x_2^{\text{inf}}(\lambda)] = [x_2(\lambda)], \end{cases} ; \quad \begin{cases} [x_1^{\text{sup}}(\lambda)] = \begin{cases} [4\lambda - 7, 3 - 10\lambda], & \text{if } 0 \leq \lambda \leq 0.5, \\ [4\lambda - 7, -1 - 2\lambda], & \text{if } 0.5 \leq \lambda \leq 1, \end{cases} \\ [x_2^{\text{sup}}(\lambda)] = \begin{cases} [6\lambda - 10, -1 - 6\lambda], & \text{if } 0 \leq \lambda \leq 0.5, \\ [2\lambda - 8, -2 - 4\lambda], & \text{if } 0.5 \leq \lambda \leq 1. \end{cases} \end{cases} \quad (40)$$

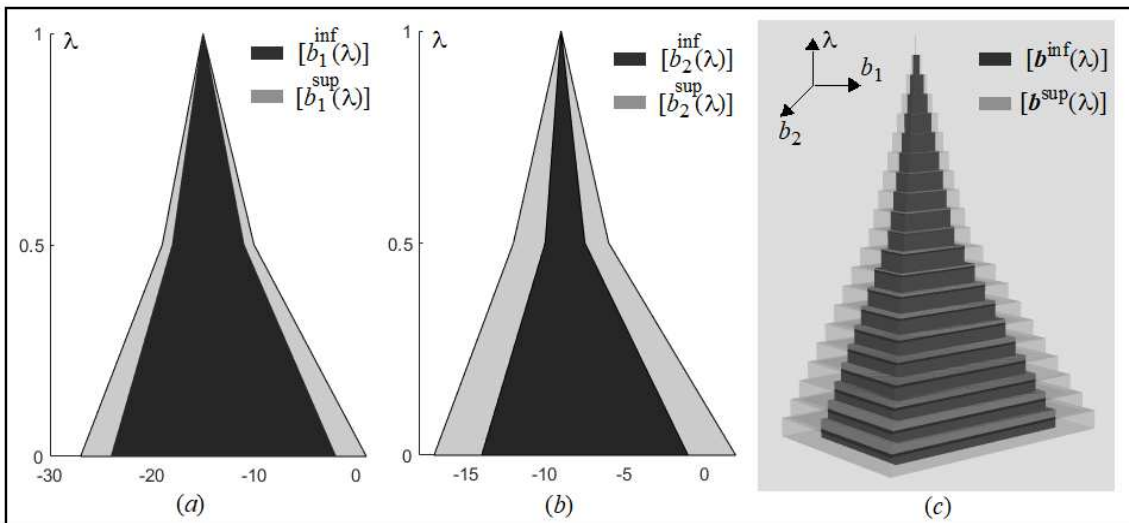


Fig. 20. Representations of IV-T2FSs and TBV-T1FS.

At each level λ , the solutions can be expressed as TIs $\llbracket x_i(\lambda) \rrbracket = \llbracket [x_i^{\text{inf}}(\lambda)], [x_i^{\text{sup}}(\lambda)] \rrbracket, i=1, 2$. As shown in Figs. 21(a) and (b), we can state that if $\llbracket x_2(\lambda) \rrbracket$ can be considered as an IV-T2FS, $\llbracket x_1(\lambda) \rrbracket$ cannot be represented by an IV-T2FS because its lower bound is not an IV-T1FS. Moreover, at each λ , these solutions can be represented by a TB $\llbracket x(\lambda) \rrbracket = \llbracket x_1(\lambda) \rrbracket \times \llbracket x_2(\lambda) \rrbracket$ in plane (x_1, x_2) . Fig. 21(c) shows that when a sampling step size of 0.05 on λ is used, the stacking of TBs $\llbracket x(\lambda) \rrbracket$ cannot be interpreted as a TBV-T1FS but as a TGB. Although the parameters of the fuzzy SoEs, i.e., (36), are IV-T2FSs (a TBV-T1FS), the solution is not a TBV-T1FS and cannot be considered as a T2FS. In this context, the TGB shown in Fig. 21(c), which is a particular case of a TGS, can be used to interpret some uncertain type-2 fuzzy SoEs whose solutions are not T2FSs.

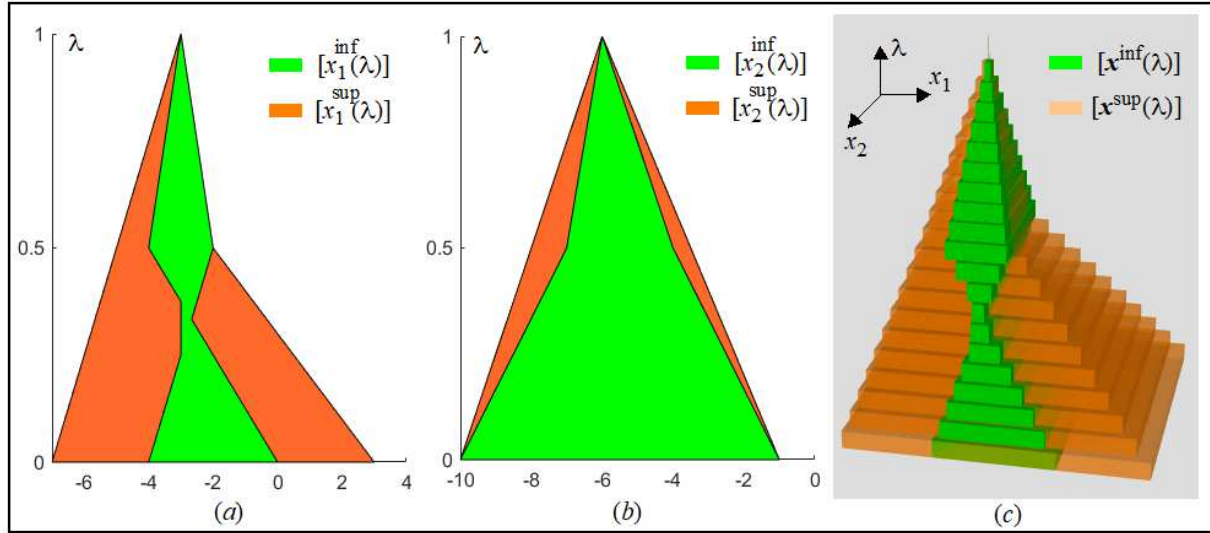


Fig. 21. 2D and 3D representations of the BV-T1FS. Algebraic solution of the system, i.e. (36).

3.1.2 Example 2

As presented in Example 1, the algebraic solution of fuzzy SoEs is restrictive or even empty. Therefore, solving (32) using an embedded approach can turn out to be unrealistic (improper IV-T1FSs, for example). Another way of solving (32), which represents a dominant approach in the literature, is based on treating the SoEs as a set of crisp SoEs whose parameters belong to the corresponding IV-T1FSs (inclusion problem). In this case, at each λ -level, SoEs are considered as interval SoEs [3][40][62][64][66], i.e.,

$$A \times x = b \text{ with } A \in [A(\lambda)] \text{ and } b \in [b(\lambda)], \forall \lambda \in [0, 1]. \quad (41)$$

Therefore, (41) interprets (32) not as a strict equality between the left- and right-hand sides but as a family of crisp SoEs $A \times x = b$ of the same structure with $A \in [A(\lambda)]$ and $b \in [b(\lambda)]$ [65]. In solving (32), the popular ideas are the concept of a united set solution (USS) and a tolerable set solution (TSS) [25][56][63][66]. USS is formalized using universal quantifier (\forall) and is defined as

$$X^{\text{USS}}(\lambda) = \{x \in \square^n \mid \forall A \in [A(\lambda)], \exists b \in [b(\lambda)], A \times x = b\}. \quad (42)$$

Equation (42) can be written as [66]

$$X^{\text{USS}}(\lambda) = \{x \in \square^n \mid \exists A \in [A(\lambda)], A \times x \in [b(\lambda)]\}. \quad (43)$$

The solution, i.e., (43), refers to understanding what the solution of the fuzzy SoEs, i.e., (32), is. This USS is a set of solutions such that at least one $A \in [A(\lambda)]$ exists in which left-hand side $A \times x$ falls into right-hand side $[b(\lambda)]$. Another solution, which is called TSS, ensures strong compatibility between the parameters and data [66]. TSS is rarely treated in a fuzzy context. It is formalized using existential quantifier (\exists) and refers to the set of solutions in which left-hand side $A \times x$ falls into right-hand side $[b(\lambda)]$ for any $A \in [A(\lambda)]$. TSS is expressed as

$$X^{\text{TSS}}(\lambda) = \{x \in \square^n \mid \forall A \in [A(\lambda)], \exists b \in [b(\lambda)], A \times x = b\}. \quad (44)$$

Equation (44) can be reformulated as

$$\mathbb{X}^{\text{TSS}}(\lambda) = \{ \mathbf{x} \in \mathbb{R}^n \mid \forall A \in [A(\lambda)], A \times \mathbf{x} \in [b(\lambda)] \}. \quad (45)$$

These two solutions can be combined and lead to a new interpretation of the solution of the fuzzy SoEs, namely, (32). Indeed, because the parameters in the left- and right-hand sides of (32) are uncertain, the set of solutions should also be uncertain. Therefore, for each level λ , the set of solutions is not CS \mathbb{X} but an uncertain set that can be represented by TS $\llbracket \mathbb{X}(\lambda) \rrbracket = \llbracket \mathbb{X}^{\text{inf}}(\lambda), \mathbb{X}^{\text{sup}}(\lambda) \rrbracket$. The bound \mathbb{X}^{inf} , which coincides with TSS, is considered as a set of certain solutions. The bound \mathbb{X}^{sup} , which refers to USS, is considered as a set of plausible solutions. Difference $\mathbb{X}^{\text{sup}} \setminus \mathbb{X}^{\text{inf}}$ represents plausible but uncertain solutions. The stacking of TSs $\llbracket \mathbb{X}(\lambda) \rrbracket$ leads to a TGS. If the monotonicity constraint, i.e., (23), is guaranteed, TGS becomes a TFS, i.e., a T2FS. In the case when $[A(\lambda)]$ is a crisp matrix, the TGS is reduced to a GS (TFS to T1FS, respectively).

Let us consider the 2×2 fuzzy linear SoEs where the elements of $[A]$ and $[b]$ are IV-T1FSs, which are defined by

$$\begin{cases} [A(\lambda)] = \begin{pmatrix} [a_{11}(\lambda)] & [a_{12}(\lambda)] \\ [a_{21}(\lambda)] & [a_{22}(\lambda)] \end{pmatrix} = \begin{pmatrix} [2+\lambda, 4-\lambda] & [-2+1.5\lambda, 1-1.5\lambda] \\ [-1+1.5\lambda, 2-1.5\lambda] & [2+\lambda, 4-\lambda] \end{pmatrix}, \\ [b(\lambda)] = \begin{pmatrix} [b_1(\lambda)] \\ [b_2(\lambda)] \end{pmatrix} = \begin{pmatrix} [-2+2\lambda, 2-2\lambda] \\ [-2+2\lambda, 2-2\lambda] \end{pmatrix}. \end{cases} \quad (46)$$

At $\lambda = 0$, (46) corresponds to the popular interval linear SoEs, which are repeatedly used by many authors (e.g. [25], [31], [36], [40], [52], and [63]). The set of solutions of (46) provided in [31], [36], [40], and [52] (for $\lambda = 0$) is a CS, which is shown in Fig. 22(a). This solution corresponds to USS produced by interval solvers such as the Intlab solver [36][52] (see <http://www.ti3.tu-harburg.de/intlab/>). Furthermore, we can state that this solution is not a box even though elements $[A(0)]$ and $[b(0)]$ are CIs. The stacking of CSs $\mathbb{X}(\lambda)$ leads to consonant GS (T1FS), as shown in Fig. 22(b), when a sampling step size of 0.1 on λ is used.

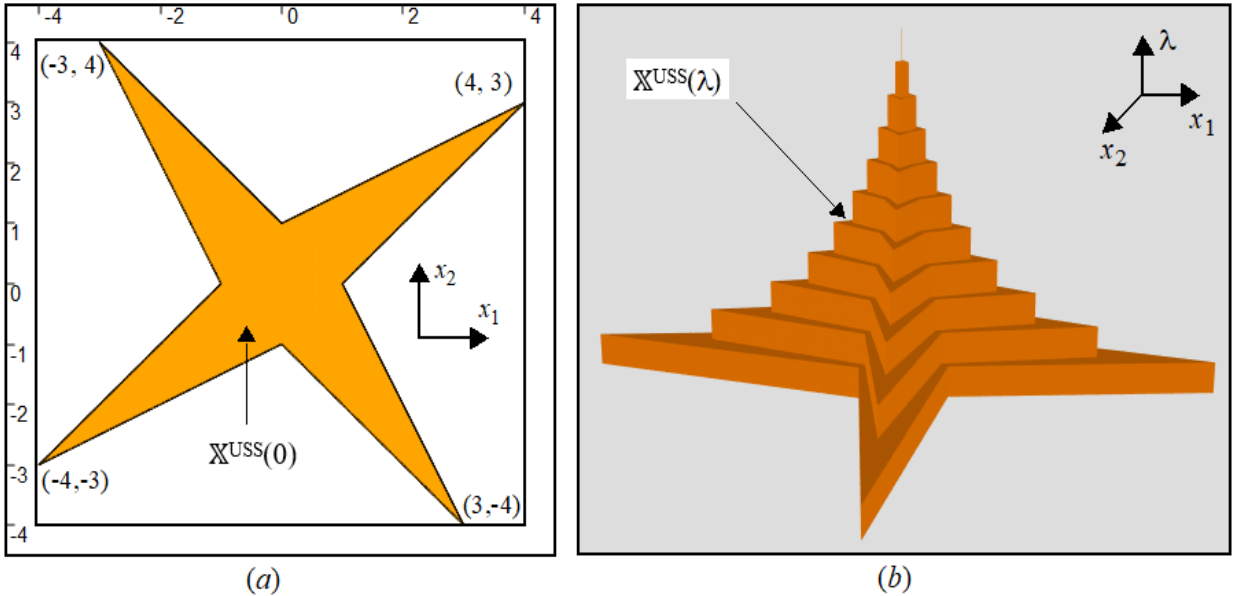


Fig. 22. Solution of SoEs, i.e., (46), using Intlab solver

This type of result is generally presented in solving fuzzy SoEs according to USS [31]. Our approach differs from those conventionally proposed in the literature. Therefore, at each level λ , the solution of (46) is not CS $\mathbb{X}(\lambda)$ but TS $\llbracket \mathbb{X}(\lambda) \rrbracket = \llbracket \mathbb{X}^{\text{inf}}(\lambda), \mathbb{X}^{\text{sup}}(\lambda) \rrbracket$. By stacking TSs $\llbracket \mathbb{X}(\lambda) \rrbracket$ according to the λ dimension, the solution is not a GS but a TGS. The certain and plausible solutions are shown in Fig. 23(a) for $\lambda = 0$. It is computed using the same methodology detailed in Sections 2.3.2 and 2.6.2, i.e.,

$$\left\{ \begin{array}{l} \mathbb{X}^{\text{sup}}(\lambda) = \{\mathbf{x} \mid \exists A \in [A(\lambda)], A \times \mathbf{x} \in [b(\lambda)]\} = \bigcap_{i,j \in \{1,2\}} \{\mathbf{x} \mid \exists a_{ij} \in [a_{ij}(\lambda)], A \times \mathbf{x} \in [b(\lambda)]\}, \\ \mathbb{X}^{\text{inf}}(\lambda) = \{\mathbf{x} \mid \forall A \in [A(\lambda)], A \times \mathbf{x} \in [b(\lambda)]\} = \bigcap_{i,j \in \{1,2\}} \{\mathbf{x} \mid \forall a_{ij} \in [a_{ij}(\lambda)], A \times \mathbf{x} \in [b(\lambda)]\} \\ = \bigcap_{i,j \in \{1,2\}} \overline{\{\mathbf{x} \mid \exists a_{ij} \in [a_{ij}(\lambda)], A \times \mathbf{x} \notin [b(\lambda)]\}}. \end{array} \right. \quad (47)$$

Solutions $\mathbb{X}^{\text{sup}}(\lambda)$ and $\mathbb{X}^{\text{inf}}(\lambda)$ are equivalent to the USS and TSS solutions proposed in [25] and [63], respectively. We can verify that GSs $\mathbb{X}^{\text{sup}}(\lambda)$ and $\mathbb{X}^{\text{inf}}(\lambda)$ obey the monotonicity condition, namely, (18), and they can be considered as T1FSs. In this case, TGS shown in Fig. 23(b) is a TFS and can be interpreted as a T2FS.

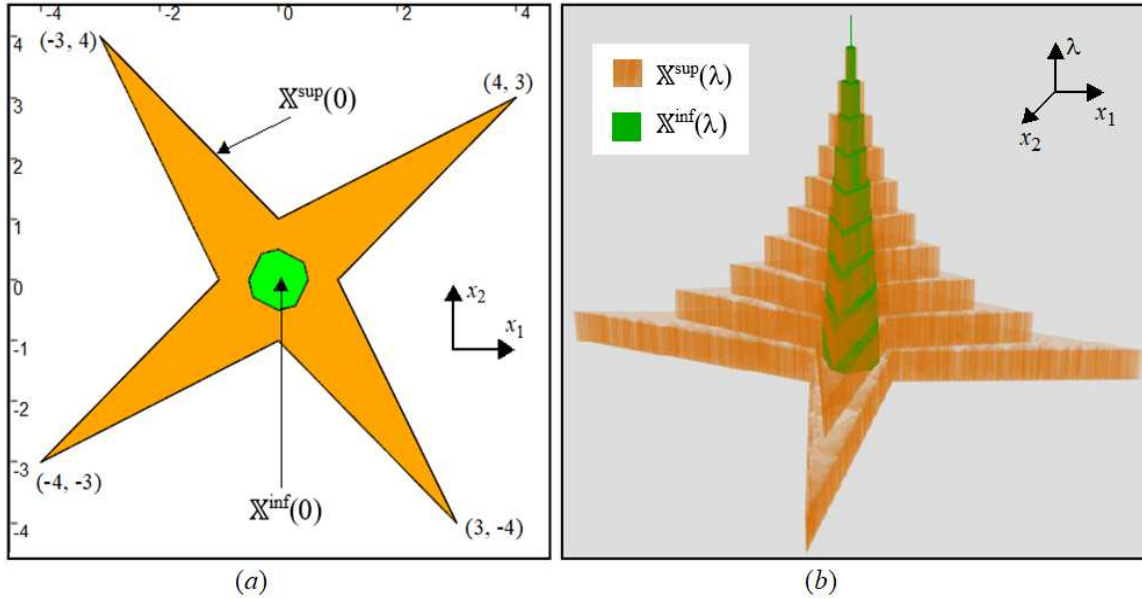


Fig. 23. TS and TGS solutions of SoEs, i.e., (46).

3.2 Uncertain fuzzy regression

In the literature, fuzzy regression has often been approached using a parametric paradigm where the estimation of the fuzzy parameters remains a major objective. Fuzzy regression is usually addressed using IV-T1FS models where the inputs, outputs, and parameters are represented by IV-T1FSs (e.g., [4], [7], [15], [21], and [23]). In this framework, the fuzzy regression can be considered as a generalization of the interval regression in which the CI specificity is enriched through the vertical λ dimension. This finding is consistent with the works published in the literature where fuzzy regression has been generally addressed as an interval regression using the concept of λ -cuts (e.g., [4], [7], [15], [21], and [23]). Therefore, fuzzy regression uses two dimensions (horizontal and vertical). The horizontal dimension is similar to that used in the interval regression. The vertical dimension is related to the relevance degrees and is limited to the unit interval $[0, 1]$ (λ -cuts).

Although significant advances have been achieved using fuzzy-regression approaches, two important considerations deserve more attention. The first consideration is related to the horizontal dimension and focuses on how to handle inputs depending on whether they are crisp or uncertain. Furthermore, in the fuzzy-regression literature, different types of data have been considered, i.e., crisp inputs/uncertain outputs (CI/UO) and uncertain inputs/uncertain outputs (UI/UO) [9][7][13][21][23]. However, both situations are approached using the same formalism, which results in the same nature, i.e., the parameters are CIs (IV-T1FSs). Nevertheless, when certain and plausible reasoning are considered, the CI/UO and UI/UO data involve two different situations and do not lead to the same results in the parameter-estimation problem. This phenomenon is illustrated in Application 3. The second consideration refers to the vertical dimension. Therefore, if the estimation

problem is addressed without any constraint of consistency between the λ levels, the results can be not nested according to the λ dimension and cannot be regarded as fuzzy quantities. This situation is illustrated in Application 4. For simplicity of illustration, the model is considered as linear. However, the approach is applicable regardless of the nonlinear form of the regression model.

3.2.1 Example 3

Let us consider the availability of a linear model $\mathcal{M}(x, \mathbf{p})$, where $\mathbf{p} = (p_1, p_2)$ is the vector of the parameters, which can fit input data x and output data y , i.e.,

$$y = \mathcal{M}(x, \mathbf{p}) = p_1 + p_2 x. \quad (48)$$

Let this model be uncertain with CI inputs $[x_i]$ and CI outputs $[y_i]$. A part of the CI input–output data set used in [7] and [16] is considered (see Table 1).

Index	Interval Input $[x_i]$	Interval Output $[y_i]$	Index	Interval Input $[x_i]$	Interval Output $[y_i]$
1	[-2.0216, -2.0129]	[3.0747, 5.5086]	11	[-1.0307, -1.0093]	[-0.2289, 1.4711]
2	[-1.9833, -1.8472]	[2.6593, 5.3167]	12	[-0.9254, -0.8637]	[-0.5381, 1.1247]
3	[-1.8708, -1.7937]	[2.1659, 4.6264]	13	[-0.8846, -0.8294]	[-0.6047, 1.0183]
4	[-1.6856, -1.6597]	[1.7191, 3.9269]	14	[-0.7296, -0.5908]	[-1.0032, 0.5606]
5	[-1.6573, -1.6264]	[1.6099, 3.8040]	15	[-0.6068, -0.5678]	[-1.0037, 0.3751]
6	[-1.5110, -1.4405]	[0.9350, 3.0874]	16	[-0.5190, -0.4943]	[-1.1321, 0.1756]
7	[-1.3539, -1.3405]	[0.6322, 2.5689]	17	[-0.3495, -0.3467]	[-1.2932, -0.1293]
8	[-1.3019, -1.1915]	[0.3766, 2.3968]	18	[-0.2990, -0.2970]	[-1.3375, -0.2122]
9	[-1.1970, -1.1836]	[0.1969, 2.0139]	19	[-0.2048, -0.1976]	[-1.4083, -0.3533]
10	[-1.0913, -1.0495]	[-0.0819, 1.6821]	20	[-0.1416, -0.1000]	[-1.4504, -0.4383]

Table 1: CI inputs and CI outputs.

In fuzzy and interval regressions, the parameter-estimation problem is traditionally approached by minimizing an objective function (with or without a penalty term and sometimes under constraints). The vector of the parameters that minimizes this objective function is viewed as the optimal one. In this framework, possibilistic and least square approaches [21][68] are the most dominant in the literature (see [17] for a good survey). In contrast to the conventional fuzzy and interval regression approaches, our approach is not based on the minimization of an objective function. Therefore, instead of determining a single optimal vector of parameters, the proposed approach aims at determining the set of all feasible vectors of parameters. Once the set of all possible parameters has been determined, practitioners can choose a vector of parameters based on a desired criterion. Therefore, our objective is to determine the set of all feasible parameters such that for inputs x_i in $[x_i]$, the outputs produced by \mathcal{M} are in $[y_i]$, i.e., $\mathcal{M}(x_i, \mathbf{p}) \in [y_i]$. To highlight the influence of uncertain inputs, we first assume that the inputs are crisp and given by their midpoints, i.e., the midpoint of $[x_i]$. In this case, the set of all feasible parameters is a CS, which is expressed as

$$\mathbb{P} = \{ \mathbf{p} = (p_1, p_2) \mid \forall x_i, i \in \{1, \dots, 20\}, \mathcal{M}(x_i, \mathbf{p}) \in [y_i] \} = \bigcap_{i \in \{1, \dots, 20\}} \{ \mathbf{p} = (p_1, p_2) \mid \forall x_i, \mathcal{M}(x_i, \mathbf{p}) \in [y_i] \}. \quad (49)$$

The set of parameters \mathbb{P} in plane (p_1, p_2) , which is obtained using the PyIbex solver, and its approximation by box $[\mathbf{p}]$ is shown in Fig. 24. Furthermore, if the CI regression approaches were used, to avoid missing feasible parameters, box $[\mathbf{p}]$, which is shown in Fig. 24(b), can be obtained. This box is an approximate solution to the parameter-estimation problem and generates a loss of information. Now, because of the uncertainties stored in the inputs (CIs), the set of parameters is no longer CS \mathbb{P} but TS $\llbracket \mathbb{P} \rrbracket = \llbracket \mathbb{P}^{\text{inf}}, \mathbb{P}^{\text{sup}} \rrbracket$, where \mathbb{P}^{inf} and \mathbb{P}^{sup} are expressed as follows:

$$\left\{ \begin{array}{l} \mathbb{P}^{\text{sup}} = \{ \mathbf{p} \mid \forall i \in \{1, \dots, 20\}, \exists x_i \in [x_i], \mathcal{M}(x_i, \mathbf{p}) \in [y_i] \} = \bigcap_{i \in \{1, \dots, 20\}} \{ \mathbf{p} \mid \exists x_i \in [x_i], \mathcal{M}(x_i, \mathbf{p}) \in [y_i] \}, \\ \mathbb{P}^{\text{inf}} = \{ \mathbf{p} \mid \forall i \in \{1, \dots, 20\}, \forall x_i \in [x_i], \mathcal{M}(x_i, \mathbf{p}) \in [y_i] \} = \bigcap_{i \in \{1, \dots, 20\}} \{ \mathbf{p} \mid \forall x_i \in [x_i], \mathcal{M}(x_i, \mathbf{p}) \in [y_i] \} \\ = \bigcap_{i \in \{1, \dots, 20\}} \overline{\{ \mathbf{p} \mid \exists x_i \in [x_i], \mathcal{M}(x_i, \mathbf{p}) \notin [y_i] \}}. \end{array} \right. \quad (50)$$

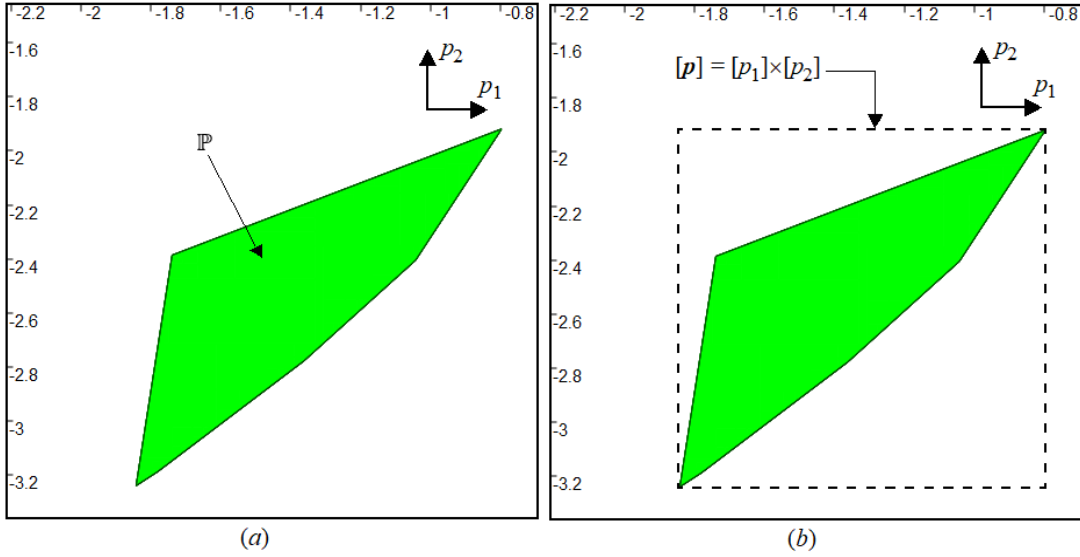


Fig. 24. Representation of CS \mathbb{P} in plane (p_1, p_2) and its approximation by box $[\mathbf{p}]$.

CS \mathbb{P}^{inf} represents a set of certain parameters, i.e., $\forall x_i \in [x_i], \mathcal{M}(x_i, \mathbf{p}) \in [y_i]$, and CS \mathbb{P}^{sup} refers to a set of plausible (possible) parameters, i.e., $\exists x_i \in [x_i], \mathcal{M}(x_i, \mathbf{p}) \in [y_i]$. CSs \mathbb{P}^{inf} and \mathbb{P}^{sup} are computed by a projection method using the PyIbex solver, as previously detailed. TS $[\mathbb{P}] = [\mathbb{P}^{\text{inf}}, \mathbb{P}^{\text{sup}}]$ in plane (p_1, p_2) is shown in Fig. 25(a). Although the inputs are uncertain (CIs), the CI regression leads to a set of parameters in the form of box $[\mathbf{p}]$, i.e., a CI for each parameter p_1 and p_2 .

For comparison purpose, when the possibilistic interval regression proposed in [7] is used, the set of parameters is box $[\mathbf{p}] = [-1.99, -0.866] \times [-3.162, -1.67]$ [see Fig. 25(a)]. This result does not introduce any specificity because of the uncertain inputs and represents only an approximation of the set of parameters. Usually, approximating uncertain solution $[\mathbb{P}] = [\mathbb{P}^{\text{inf}}, \mathbb{P}^{\text{sup}}]$ is always possible using TB $[\mathbb{p}] = [[\mathbf{p}^{\text{inf}}], [\mathbf{p}^{\text{sup}}]]$, as shown in Fig. 25(b). However, this approximation implies a loss in information.

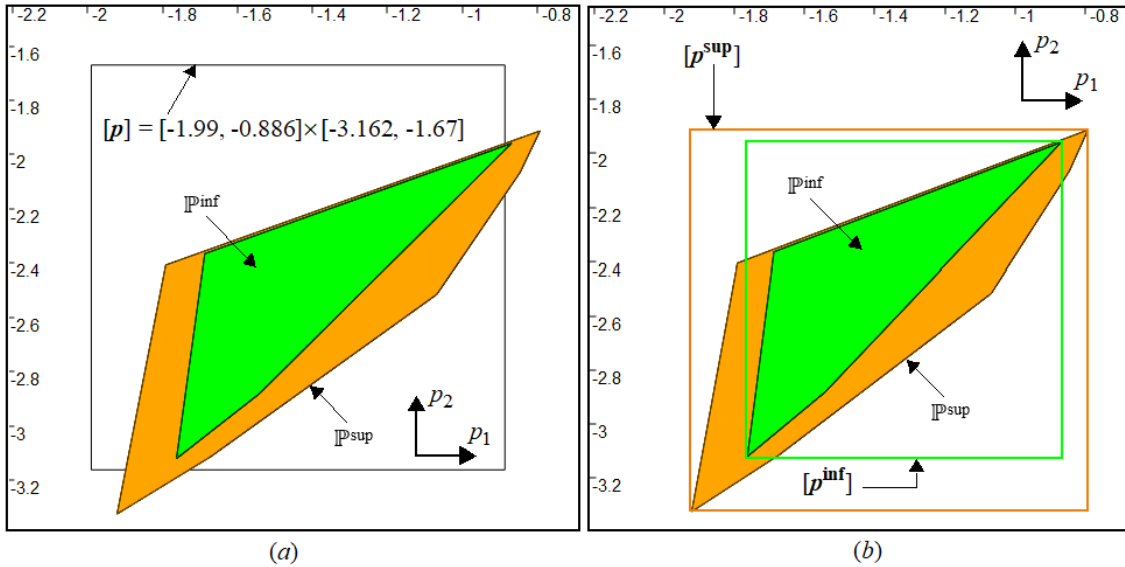


Fig. 25. Representation of TS $[\mathbb{P}]$ in plane (p_1, p_2) and its approximation using TB $[\mathbb{p}]$.

3.2.2 Example 4

Let us consider again the linear model, i.e., (48). Let us assume that this model remains uncertain with fuzzy inputs/outputs that are represented by IV-T1FSs. A process is realized where at fuzzy input $[x_i(\lambda)]$, a fuzzy output $[y_i(\lambda)]$ is collected. This process is repeated five times. The data are listed in Table 2 where the inputs are triangular IV-T1FSs and the outputs are trapezoidal IV-T1FSs.

i	$[x_i(\lambda)]$	$[y_i(\lambda)]$
1	$[0.5+0.1\lambda, 0.7-0.1\lambda]$	$[5+2\lambda, 12-\lambda]$
2	$[1.25 + 0.25\lambda, 1.75-0.25\lambda]$	$[9+2\lambda, 23-4\lambda]$
3	$[2+0.5\lambda, 3-0.5\lambda]$	$[18+2\lambda, 40-7\lambda]$
4	$[3+0.5\lambda, 4-0.5\lambda]$	$[23+4\lambda, 48-4\lambda]$
5	$[3.5+0.5\lambda, 4.5-0.5\lambda]$	$[26+4\lambda, 54-5\lambda]$

Table 2: Triangular fuzzy inputs and trapezoidal fuzzy outputs.

Because of the uncertainties stored in the inputs, at each λ level, the set of parameters is no longer CS $\mathbb{P}(\lambda)$ but TS $\llbracket \mathbb{P}(\lambda) \rrbracket = \llbracket \mathbb{P}^{\text{inf}}(\lambda), \mathbb{P}^{\text{sup}}(\lambda) \rrbracket$, where $\mathbb{P}^{\text{inf}}(\lambda)$ and $\mathbb{P}^{\text{sup}}(\lambda)$ are expressed as

$$\left\{ \begin{array}{l}
 \mathbb{P}^{\text{sup}}(\lambda) = \{ \mathbf{p}(\lambda) \mid \forall i \in \{1, \dots, 5\}, \exists x_i \in [x_i(\lambda)], \mathcal{M}(x_i, \mathbf{p}(\lambda)) \in [y_i(\lambda)] \} \\
 \quad = \bigcap_{i \in \{1, \dots, 5\}} \{ \mathbf{p}(\lambda) \mid \exists x_i \in [x_i(\lambda)], \mathcal{M}(x_i, \mathbf{p}(\lambda)) \in [y_i(\lambda)] \}, \\
 \mathbb{P}^{\text{inf}}(\lambda) = \{ \mathbf{p}(\lambda) \mid \forall i \in \{1, \dots, 5\}, \forall x_i \in [x_i(\lambda)], \mathcal{M}(x_i, \mathbf{p}(\lambda)) \in [y_i(\lambda)] \} \\
 \quad = \bigcap_{i \in \{1, \dots, 5\}} \{ \mathbf{p}(\lambda) \mid \forall x_i \in [x_i(\lambda)], \mathcal{M}(x_i, \mathbf{p}(\lambda)) \in [y_i(\lambda)] \} \\
 \quad = \bigcap_{i \in \{1, \dots, 5\}} \overline{\{ \mathbf{p}(\lambda) \mid \exists x_i \in [x_i(\lambda)], \mathcal{M}(x_i, \mathbf{p}(\lambda)) \notin [y_i(\lambda)] \}},
 \end{array} \right. \quad (51)$$

where $\mathbf{p}(\lambda) = (p_1(\lambda), p_2(\lambda))$. For instance, TSs $\llbracket \mathbb{P}(\lambda) \rrbracket = \llbracket \mathbb{P}^{\text{inf}}(\lambda), \mathbb{P}^{\text{sup}}(\lambda) \rrbracket$ for $\lambda = 0$ and $\lambda = 1$ in plane (p_1, p_2) are shown in Fig. 26. Furthermore, our method can be applied regardless of the value of λ . According to these results, we can state that if the inputs are uncertain (fuzzy), the set of parameters is a TS [see Fig. 26(a)]. However, if the input is crisp (at $\lambda = 1$ because the inputs are triangular IV-TIFSs), the set of parameters is a CS, i.e., $\mathbb{P}^{\text{inf}}(1) = \mathbb{P}^{\text{sup}}(1) = \mathbb{P}(1)$ [see Fig. 26(b)]. The superposition of CSs $\mathbb{P}^{\text{inf}}(\lambda)$ and $\mathbb{P}^{\text{sup}}(\lambda)$ (each is separately considered) leads to that shown in Fig. 27. The stacking of TSs $\llbracket \mathbb{P}(\lambda) \rrbracket$ leads to TGS, which is shown in Fig. 28, using a sampling step size of 0.1 on λ .

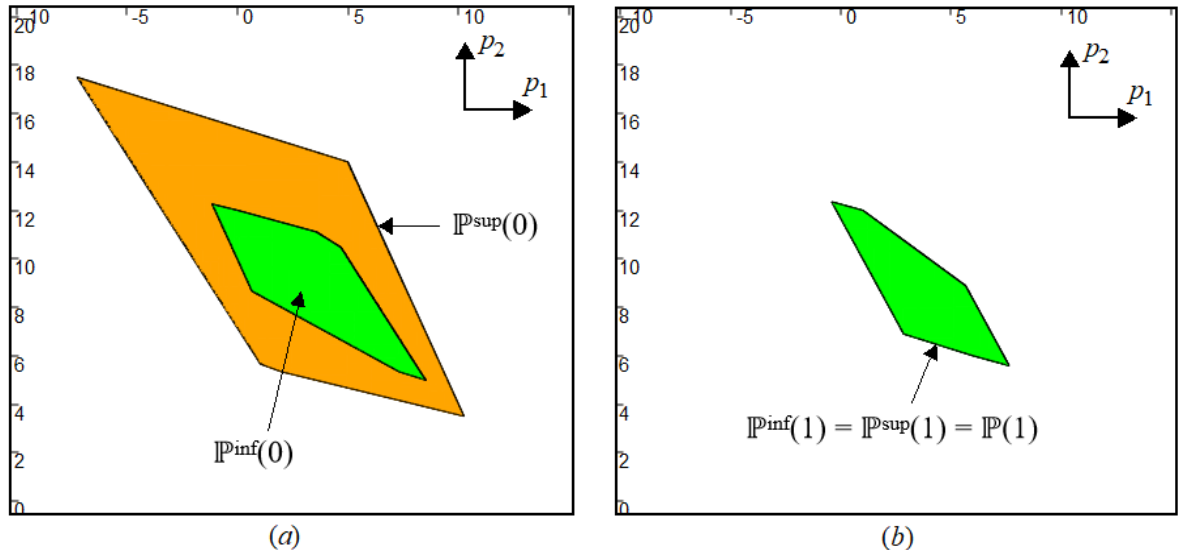


Fig. 26. TSs $\llbracket \mathbb{P}(\lambda) \rrbracket$ for $\lambda = 0$ and $\lambda = 1$ in plane (p_1, p_2) .

Fig. 27 shows that GS $\mathbb{P}^{\text{sup}}(\lambda)$ satisfies the consistency condition, namely, (18), and can be regarded as a T1FS. In contrast, GS $\mathbb{P}^{\text{inf}}(\lambda)$ is pure GS and cannot be represented by a T1FS [see Fig. 27(a), where GSs are illustrated for three values of λ]. In this case, TGS shown in Fig. 28 cannot be considered as a T2FS because the lower bound is not a T1FS.

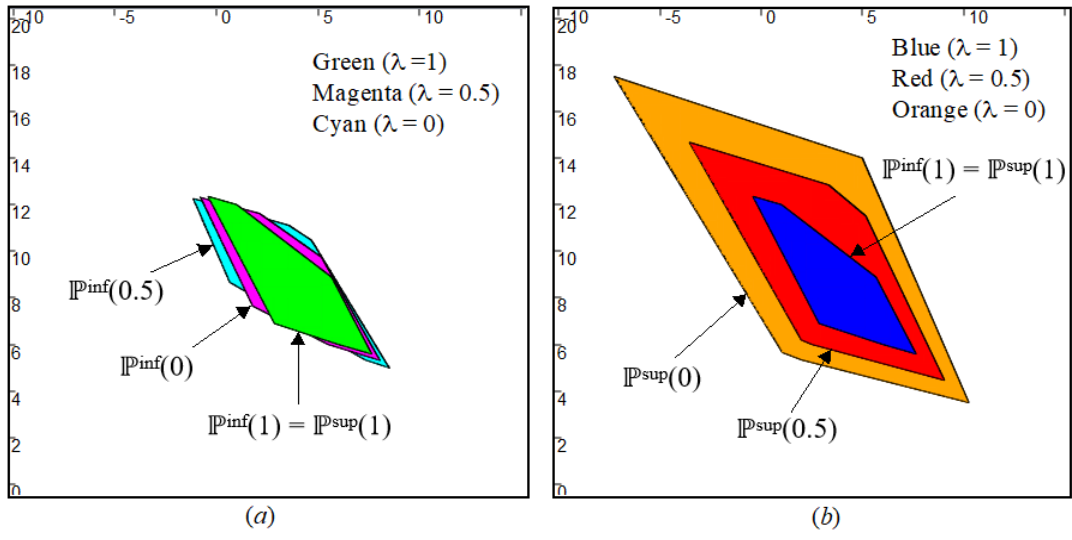


Fig. 27. GSs $\mathbb{P}^{\text{inf}}(\lambda)$ and $\mathbb{P}^{\text{sup}}(\lambda)$ for $\lambda = 0, 0.5, \text{ and } 1$.

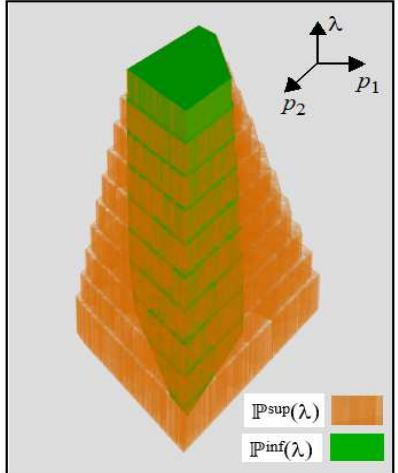


Fig. 28. TGS $\mathbb{P}(\lambda)$ using a sampling step size of 0.1 on λ .

4 Application to a real-world underwater robot

In this section, an application of the TGS concept is provided through a real experiment using the Daurade underwater robot (see Fig. 29 for Daurade and its main characteristics). The Daurade robot was built by ECA robotics and used by Direction Générale de l’Armement–Techniques Navales–French Army and Service Hydrographique et Océanographique de la Marine to perform Rapid Environment Assessment (REA) missions.

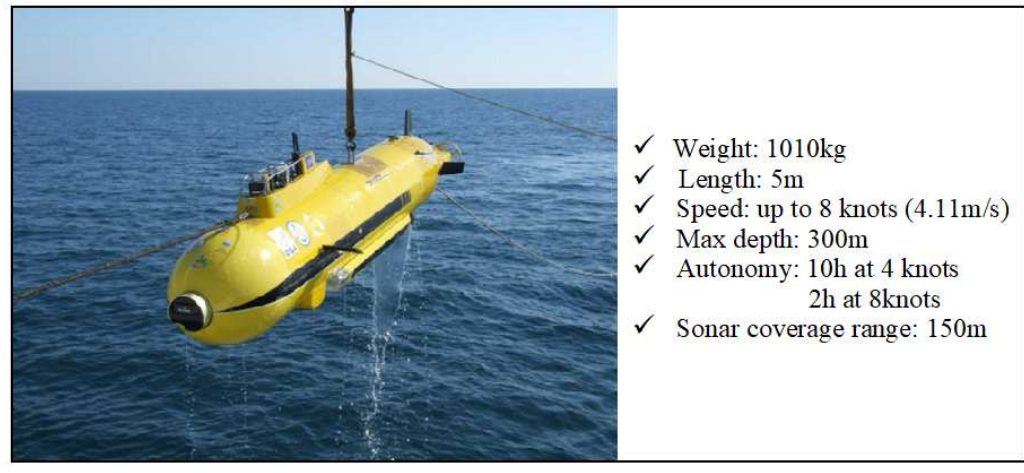


Fig. 29. Daurade underwater robot and its characteristics.

REA is designed to survey the environmental conditions of a particular location to identify any existing or potential dangers. **The objective of this application is to determine the zone explored by the Daurade robot in an uncertain environment.** The Daurade mission is related to the counter-mine warfare context where the objective is to map the seafloor using acoustic sensors. The main objective of the REA missions is to determine if the area of interest has been completely explored. Therefore, Daurade is equipped with a side scan sonar (Klein 5500), which is used to detect potential mines. Owing to this sonar, data are recorded on a line perpendicular to the path of the sensor, and images are formed by drawing these lines side by side. The portside lateral sonar antenna corresponds to a 1-m black segment at the bottom left of the robot. The approach proposed in this paper is used to validate that the zone to be explored is totally covered. **For safety reasons, the application aims at covering the total seafloor that is visible by sonar, which considers all uncertain trajectories of the robot. The uncertainty of the trajectories is induced by some disturbances such as noise sensors in a hostile environment, ocean currents, and weather conditions.**

Daurade is an autonomous underwater vehicle (AUV). An AUV is a type of intelligent robot that works in underwater conditions [32]. Daurade is equipped with an embedding localization system. Therefore, in its navigation under the surface, Daurade does not receive any electromagnetic waves. In this case, global-navigation-satellite systems, which are often used in terrestrial and aerial applications, cannot be applied in the underwater situation. In the present study, during a navigation mission, the depth is assumed to be fixed, and the position of Daurade is given by its 2D horizontal coordinates $\mathbf{x} = (x_1, x_2)$. This position is delivered through an embedded system that integrates an inertial navigation system (INS) coupled with a Doppler Velocity Log (DVL) sensing speed. Once under water, no GPS data are available, and the estimated position of the robot drifts with time. Therefore, because of disturbances, Daurade is subjected to drifting effects on its speed and consequently its position.

4.1 Application context

The application proposed in this paper is a mission of 46 min, which has been performed in the Roadstead of Brest (Brittany, France) using Daurade. It realizes a classical survey pattern composed of a set of parallel tracks at a depth of approximately 10 m. At the beginning of the mission, the robot position is exactly known owing to GPS localization. Initial condition $\mathbf{x}(0)$ is assumed equal to $(0, 0)$. Coordinates $(0, 0)$ for (x_1, x_2) are considered as our navigation origin.

The Daurade robot is controlled to follow the ideal 2D desired trajectory shown in Fig. 30(a) (solid line). In this case, when the robot dives under the surface, it does not receive electromagnetic waves anymore, and GPS cannot be considered.

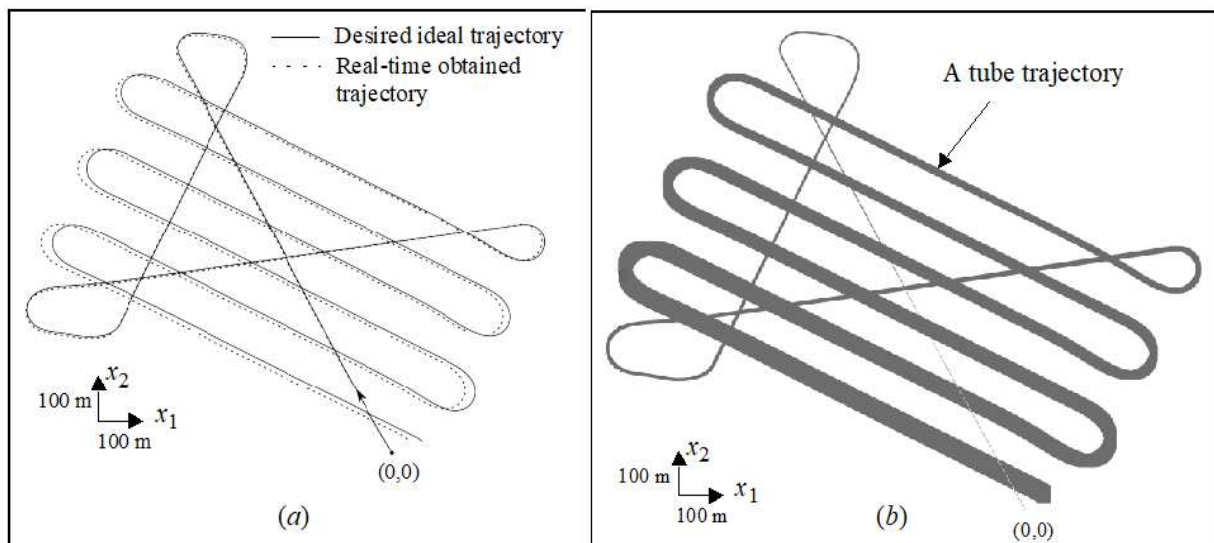


Fig. 30. Daurade trajectories. (a) 2D Crisp trajectories. (b) 2D tube trajectory (uncertain trajectory).

Daurade can estimate its successive positions using INS, which is coupled to a DVL sensing speed. However, because of some disturbances (noise sensors, ocean currents, and weather conditions), the robot is subjected to some drifting effects on its speed, its heading, and consequently its position. For instance, an experiment process has led to the trajectory shown in Fig. 30(a) (dashed line). Therefore, uncertainties (errors) in the robot trajectory are induced by the speed- and heading-drift effects. For instance, when a drift on the speed of up to $\pm 0.2\%$ is considered, the 2D robot trajectory shown in Fig. 30(a) (solid line) becomes uncertain and can be represented by a 2D tube [60] [see Fig. 30(b)].

The 2D tube shown in Fig. 30(b) represents all possible trajectories of the robot when the speed error is within the interval $[-0.2\%, +0.2\%]$. In this framework, for any considered operating conditions that are compatible with a speed drift of $\pm 0.2\%$, this tube certainly follows the true trajectory. Because the position of Daurade is obtained by integration of its speed, the uncertainty of the trajectory can normally increase over time. We must note that trajectories in the tube that are not realizable by the robot may exist.

A tube over domain $[t_0, t_f]$ can be regarded as a family (envelope or interval) of dynamic trajectories $\mathbf{x}(\cdot)$ [60]. The dot notation (\cdot) is used to distinguish between a whole trajectory $\mathbf{x}(\cdot)$ from a local evaluation $\mathbf{x}(t)$. Therefore, a tube that is denoted as $[\mathbf{x}](\cdot) = [\mathbf{x}^-(\cdot), \mathbf{x}^+(\cdot)]$ is an interval of trajectories $\mathbf{x}(\cdot)$ such that

$$\mathbf{x}^-(t) \leq \mathbf{x}^+(t), \forall t \in [t_0, t_f] \quad (52)$$

An example of a 1D tube $[x](\cdot)$ is shown in Fig. 31 with its interval bounds and an arbitrary possible trajectory $x(t)$.

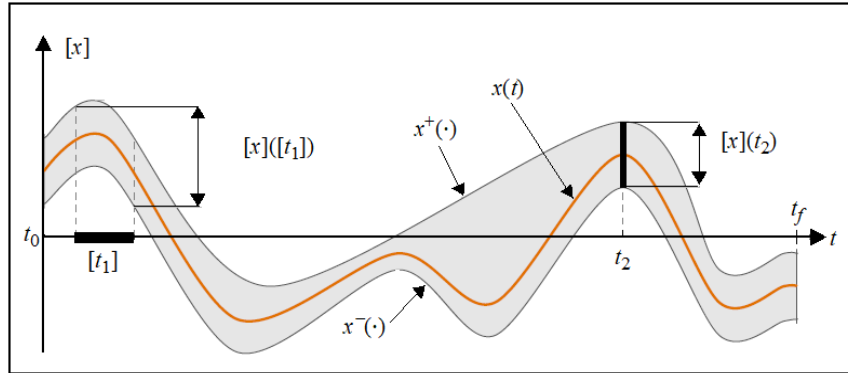


Fig. 31. Representation of a 1D tube.

Because uncertain real parameters x are represented by intervals $[x]$ and uncertain vectors \mathbf{x} are represented by boxes $[\mathbf{x}]$, the uncertain trajectories are represented by tubes $[\mathbf{x}](\cdot)$. A trajectory $\mathbf{x}(\cdot)$ belongs to tube $[\mathbf{x}](\cdot)$ if $\forall t \in [t_0, t_f], \mathbf{x}(\cdot) \in [\mathbf{x}](\cdot)$.

4.2 Trajectory uncertainty formalization

First, only the speed drifts are considered. The other drifts will be discussed later. Therefore, to determine the uncertainties related to the speed drift, experiments are performed under adverse (pessimistic) and favorable (optimistic) operating conditions. In the pessimistic case, a drift of up to $\pm 1\%$ on the robot speed is observed. In the optimistic case, the speed drift is limited to $\pm 0.2\%$. In the pessimistic case, the speed data are most imprecise but contain the highest degree of certainty, i.e., a degree of confidence $1 - \lambda = 1$ (level $\lambda = 0$). However, the optimistic situation indicates that the data are most precise but contains the highest degree of uncertainty. This case refers to $\lambda = 1$ (zero confidence level). For simplicity of implementation, the evolution between levels $\lambda = 0$ and $\lambda = 1$ is assumed to be linear. This assumption is only an approximation, and supplementary information can be used to improve this assumption. Therefore, the uncertainty related to the speed drift (speed error) is characterized by a distribution of possibility which is represented by trapezoidal IV-T1FS [4]:

$$[E_{speed}(\lambda)] = [-0.01 + 0.008\lambda, 0.01 - 0.008\lambda] \quad (53)$$

IV-T1FS $[E_{speed}(\lambda_i)]$, which is shown in Fig. 32, can be considered as a set of nested confidence intervals. The degree of necessity for CI $[E_{speed}(\lambda_i)]$ to contain the value of E_{speed} is $N([E_{speed}(\lambda_i)]) = 1 - \lambda_i$. Therefore, the confidence interval $[E_{speed}(\lambda_i)]$ is interpreted as follows: “I am certain to a $(1 - \lambda_i)$ degree that E_{speed} is in $[E_{speed}(\lambda_i)]$.” We can easily show that degree of possibility $\Pi([E_{speed}(\lambda_i)]) = 1$. More generally, a set of nested confidence intervals $[E_{speed}(\lambda_i)]$ with degrees of certainty $(1 - \lambda_i)$ is equivalent to a distribution of possibility. For each level λ , $[E_{speed}(\lambda)]$ is an interval, and the 2D horizontal robot coordinates depend on λ and is denoted by $x_\lambda = (x_1^\lambda, x_2^\lambda)$. In this case, the robot trajectory is uncertain and is represented by tube $[x_\lambda](\cdot)$ [see Fig. 33].

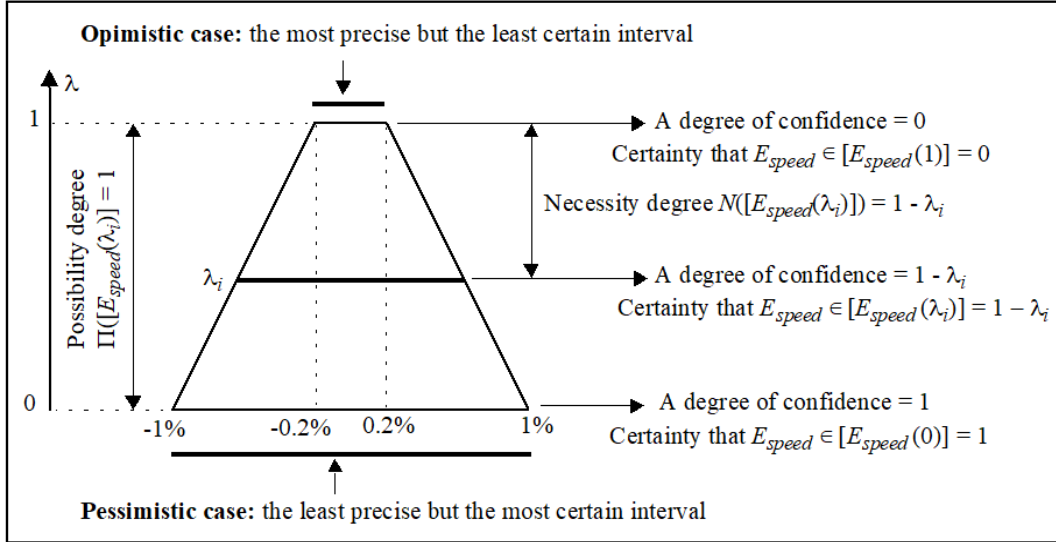


Fig. 32. IV-T1FS representing speed error $[E_{speed}(\lambda)]$.

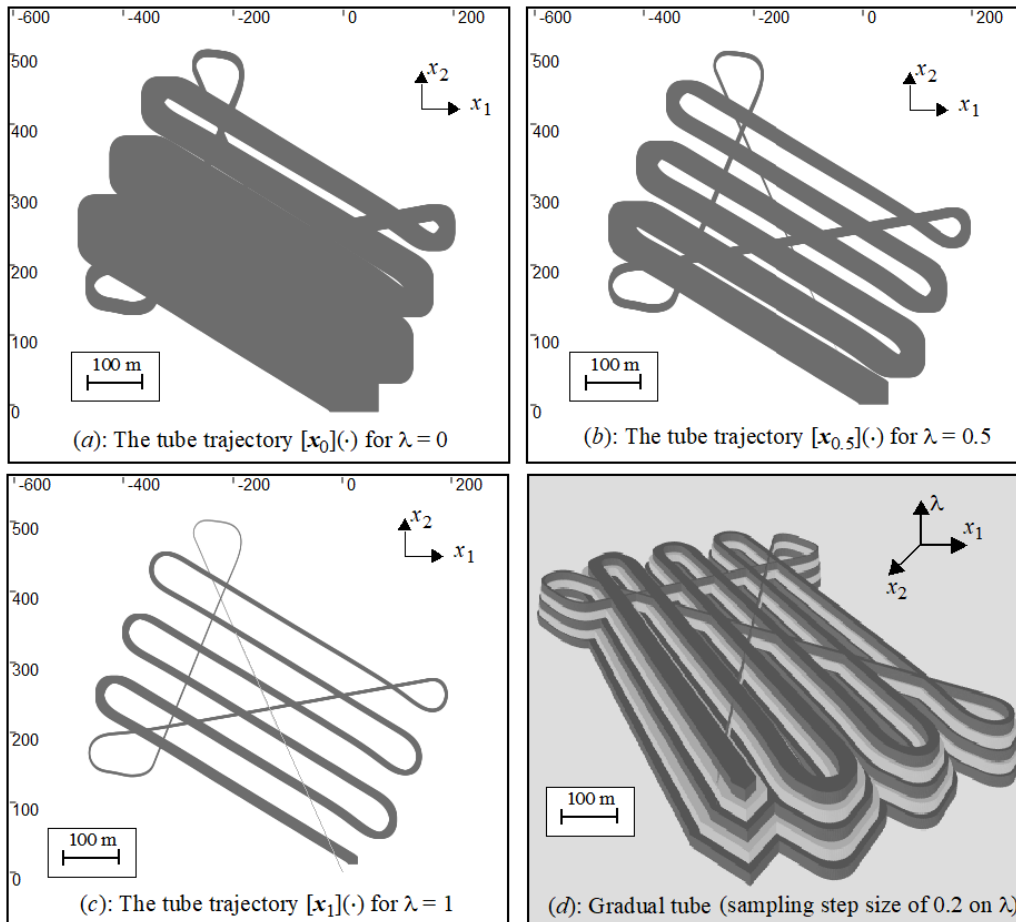


Fig. 33. Daurade tube trajectories and a gradual tube $[x_\lambda](\cdot)$ (due to the speed drifts).

The initial condition is always assumed to be equal to $(0, 0)$ irrespective of the value of λ . For example, 2D tubes trajectories $[x_\lambda](\cdot)$ induced by the speed drift at $\lambda = 0, 0.5$, and 1 are shown in Fig. 33. By integrating dimension $\lambda \in [0, 1]$, the stacking of the tubes leads to a gradual tube, which is shown in Fig. 33(d), when a sampling step size of 0.2 on λ is used. This gradual tube can be considered as an object that integrates all possible tube trajectories according to confidence degree λ .

4.3 Uncertain explored zone induced by speed drifts

The objective presented in this section is the characterization of the explored (visible) zone when the robot evolves in a gradual tube. The purpose of the characterization of this zone is to detect the presence of dangerous objects such as underwater mines. During its navigation, the robot is equipped with a scanner to observe a part of its environment. When a degree of confidence is specified (a given value of λ), a subset of the seafloor exists at each time, which is denoted by $V(x_\lambda(t)) \subset \mathbb{R}^2$, that is visible by the robot (at each time, the visibility zone can be considered as a disk around the robot position). When the robot trajectory is crisp, the explored zone can be considered as CS \mathbb{Z} , which is expressed as

$$\mathbb{Z} = \bigcup_{t \geq 0} V(x_\lambda(t)). \quad (54)$$

Equation (54) refers to the union of all disks around the dynamic robot position. Conventionally, the robot trajectory is considered as crisp. However, this crisp trajectory rarely corresponds to the observed reality because of the drifts in the robot position. In this case, the characterized navigation zone does not reflect reality, and no reliability can be associated with it. However, and in contrast to the conventional approaches, all possible trajectories are considered in our approach. Thus, because of the uncertainty in the trajectory (the robot is assumed to evolve in the tube), the explored zone becomes an uncertain set, i.e., TS $[[\mathbb{Z}(\lambda)]] = [[\mathbb{Z}^{\text{inf}}(\lambda), \mathbb{Z}^{\text{sup}}(\lambda)]]$, whose bounds are computed using

$$\begin{cases} \mathbb{Z}^{\text{sup}}(\lambda) = \bigcup_{x_\lambda(\cdot) \in [x_\lambda](\cdot)} \bigcup_{t \geq 0} V(x_\lambda(t)), \\ \mathbb{Z}^{\text{inf}}(\lambda) = \bigcap_{x_\lambda(\cdot) \in [x_\lambda](\cdot)} \bigcup_{t \geq 0} V(x_\lambda(t)). \end{cases} \quad (55)$$

In (55), $\mathbb{Z}^{\text{inf}}(\lambda)$ is called the certainly explored zone (lower bound). It corresponds to the set of all points in the seafloor that have certainly been observed by sonar irrespective of the position of the robot in its tube (for all feasible trajectories). In the same manner, $\mathbb{Z}^{\text{sup}}(\lambda)$, which represents the explored plausible zone (upper bound), refers to the set of all points in the seafloor that have been observed by sonar for some feasible trajectories and unobserved by it in some other feasible trajectories. Moreover, the points that are outside $\mathbb{Z}^{\text{sup}}(\lambda)$ are certainly not observed by the sonar. Points in penumbra $\mathbb{Z}^{\text{sup}}(\lambda) \setminus \mathbb{Z}^{\text{inf}}(\lambda)$ are possibly (but not certainly) observed by the sonar. Tube $[x_0](\cdot)$ shown in Fig. 33 indicates the least precise but the most certain observation. In contrast, tube $[x_1](\cdot)$ is the most precise but the least certain observation. Therefore, the confidence degree associated with each tube $[x_\lambda](\cdot)$ is $(1-\lambda)$. By separately considering certain zone $\mathbb{Z}^{\text{inf}}(\lambda)$ or plausible zone $\mathbb{Z}^{\text{sup}}(\lambda)$, each of these zones is a CS at each level λ . For example, $\mathbb{Z}^{\text{inf}}(0)$ and $\mathbb{Z}^{\text{sup}}(0)$ are shown in Fig. 34. Furthermore, in the absence of uncertainty where the robot trajectory is known, the explored zone becomes a unique CS, i.e., $\mathbb{Z}^{\text{inf}} = \mathbb{Z}^{\text{sup}} = \mathbb{Z}$.

The stacking of CSs $\mathbb{Z}^{\text{sup}}(\lambda)$ and $\mathbb{Z}^{\text{inf}}(\lambda)$ according to the λ dimension (each of them separately considered) leads to GSs shown in Fig. 35. We can state that these GSs obey the monotonicity (consistency) condition, i.e., (18), and can be regarded as TIFSs.

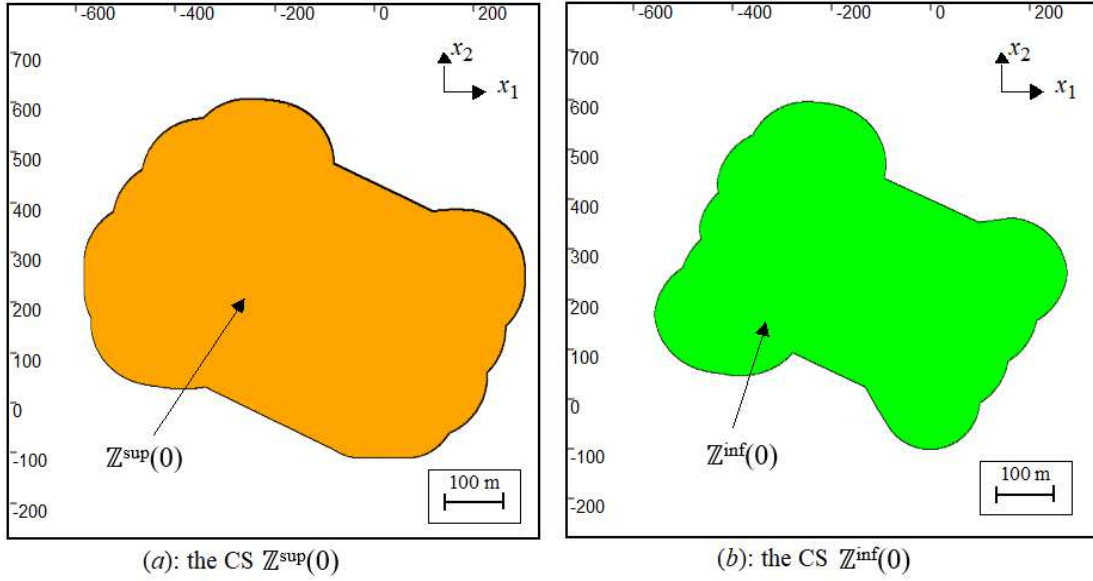


Fig. 34. Lower and upper explored zones $Z^{\text{inf}}(0)$ and $Z^{\text{sup}}(0)$.

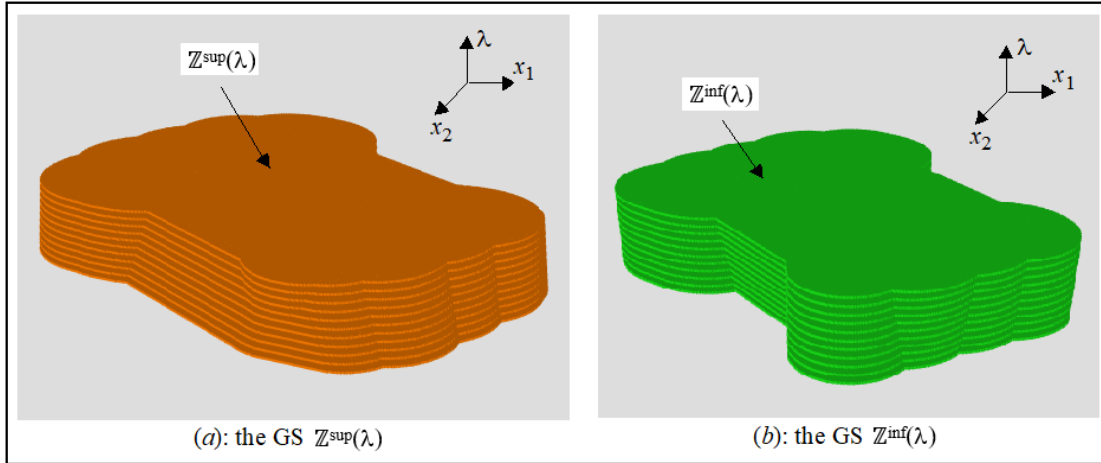


Fig. 35. Discrete representation of GSs $Z^{\text{inf}}(\lambda)$ and $Z^{\text{sup}}(\lambda)$ using a sampling step size of 0.1 on λ .

Furthermore, for a given level λ , merging two lower and upper CSs $Z^{\text{inf}}(\lambda)$ and $Z^{\text{sup}}(\lambda)$ into a single entity results in an uncertain explored zone, which is represented by TS $\llbracket Z(\lambda) \rrbracket = \llbracket Z^{\text{inf}}(\lambda), Z^{\text{sup}}(\lambda) \rrbracket$. For example, the resulting TSs at $\lambda = 0, 0.5$, and 1 are shown in Figs. 36(a)–(c), respectively.

Moreover, TGS shown in Fig. 36(d) is obtained by the stacking of TSs according to the λ dimension when a sampling step size of 0.1 on λ is used. This result could also have resulted from the fusion of GSs shown in Fig. 35 in a unique entity, i.e., TGS. In this case, because lower and upper GSs are T1FSs, the TGS is a TFS, which can be considered as a T2FS.

Without going into some details, which are protected for confidentiality reasons, the usefulness of this approach fits into a risk decision-making strategy in an uncertain environment where zones $Z^{\text{sup}}(\lambda)$ and $Z^{\text{inf}}(\lambda)$ can be considered as the higher and lower bounds of uncertainty in the decision process. Therefore, a TGS can be considered as a cartography which associates with each degree λ , a certain (safest) zone $Z^{\text{inf}}(\lambda)$, and a plausible safe zone $Z^{\text{sup}}(\lambda)$. Thus, decision makers use some degree of confidence in formulating their decisions on the safety of the submarine navigation (exploration) zone. Because $Z^{\text{sup}}(\lambda)$ and $Z^{\text{inf}}(\lambda)$ are T1FSs, the certainty and reliability of the decision can be quantified using the possibility theory [7]. Therefore, for chosen degree λ_i , which depends on the operating conditions (weather, sea currents, etc.), the degree of necessity for $Z^{\text{inf}}(\lambda)$ is $1-\lambda_i$. For instance, a decision maker can affirm that “I am certain to a $(1-\lambda_i)$ degree that certain zone $Z^{\text{inf}}(\lambda)$ is safe.” The same remark can be made on plausible zone $Z^{\text{sup}}(\lambda)$. From the methodological

perspective, we must note that the difference that can be achieved between TGSs and GSs is similar to the difference that can be obtained between T2FSs and T1FSs. Furthermore, in the TGS representation, no consistency constraint is imposed for GSs. Therefore, TGSs can be used to represent some uncertain quantities that are impossible to represent by T2FSs. This point will be illustrated in the next section.

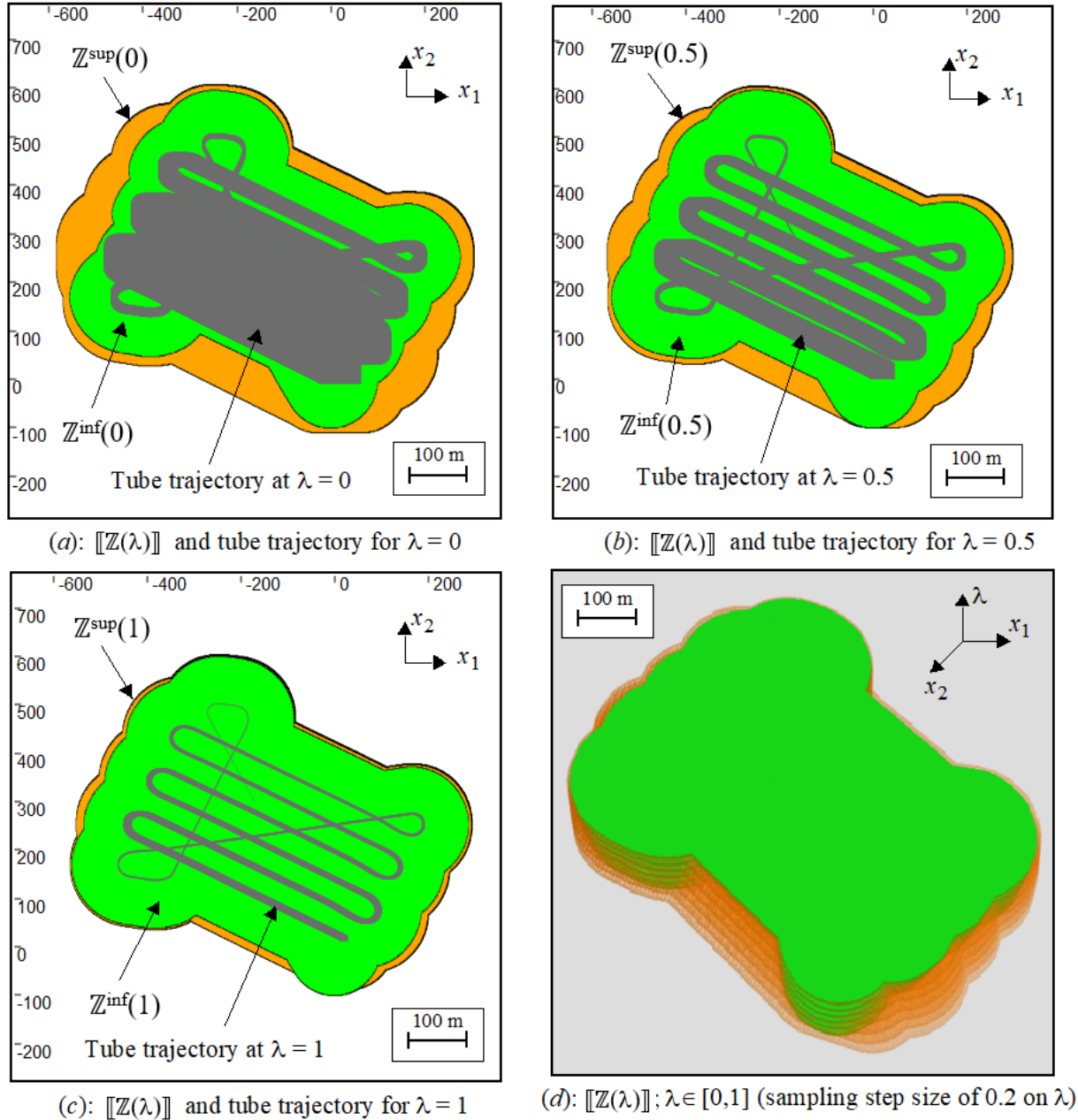


Fig. 36. TSs and TGS representations (according to the speed drifts).

4.4 Uncertain explored zone induced by speed and heading drifts

In addition to the speed drifts shown by IV-T1FS in Fig. 32, we will consider the heading drifts. To determine the uncertainty according to the heading drifts, the same methodology presented in Section 4.2 is adopted where pessimistic and optimistic operating conditions are considered. In the pessimistic situation, a drift of up to $\pm 1.5\%$ has been observed on the robot heading. In the optimistic case, the heading drift is limited to $\pm 0.3\%$. In this case, the uncertainty (error) related to the heading drifts is represented by trapezoidal IV-T1FS, i.e.,

$$[E_{\text{heading}}(\lambda)] = [-0.015 + 0.012\lambda, 0.015 - 0.012\lambda]. \quad (56)$$

For each level λ , the underwater robot trajectory is in its tube. This induces an uncertain zone that is represented by a TS, as shown in Fig. 37, at $\lambda = 0, 0.5$, and 1.

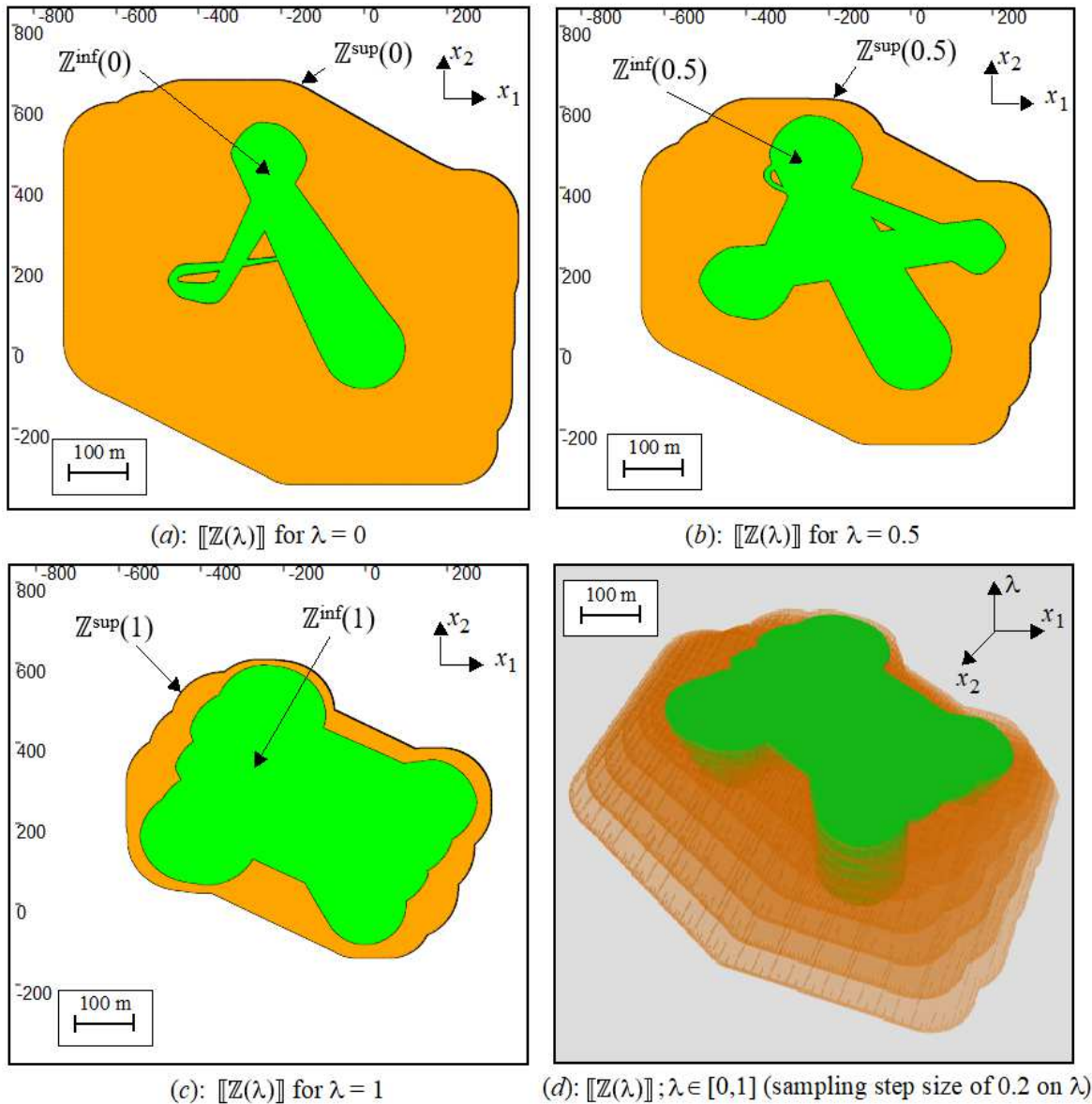


Fig. 37. TSs and TGS representations (due to the speed and heading drifts).

Furthermore, 2D tube trajectories $[x_\lambda](\cdot)$ induced by the speed and heading drifts at $\lambda = 0$ and $\lambda = 1$ are shown in Fig. 38, which shows that the double uncertainty (speed and heading uncertainties) implies a large width of the tubes and, consequently, a significant overlap in the trajectories. The stacking of these TSs leads to TGS, which is shown in Fig. 37(d). According to these results, we can verify that if $Z^{\text{sup}}(\lambda)$ is nested according to λ , $Z^{\text{inf}}(\lambda)$ is not nested, and it does not obey the consistency constraint [see Fig. 39(b)]. Therefore [and as shown in Fig. 39(a)], we can observe that $Z^{\text{inf}}(1) \not\subset Z^{\text{inf}}(0)$. This non-nesting phenomenon provides the GS and TGS concepts their full meanings. In this case, the TGS, which is shown in Fig. 37(d), is an uncertain quantity that cannot be represented by a T2FS.

In this context, TGS shown in Fig. 37(d) can always be considered as a cartography that associates with each degree λ , a certain safe explored zone $Z^{\text{inf}}(\lambda)$, and a plausible safe explored zone $Z^{\text{sup}}(\lambda)$. However, the quantification of uncertainty using the possibility theory requires GSs to be represented by T1FSs that are considered as distributions of possibility. Therefore, in a pure gradual

framework, the uncertainty cannot be quantified using the possibility measures but in terms of belief functions [7].

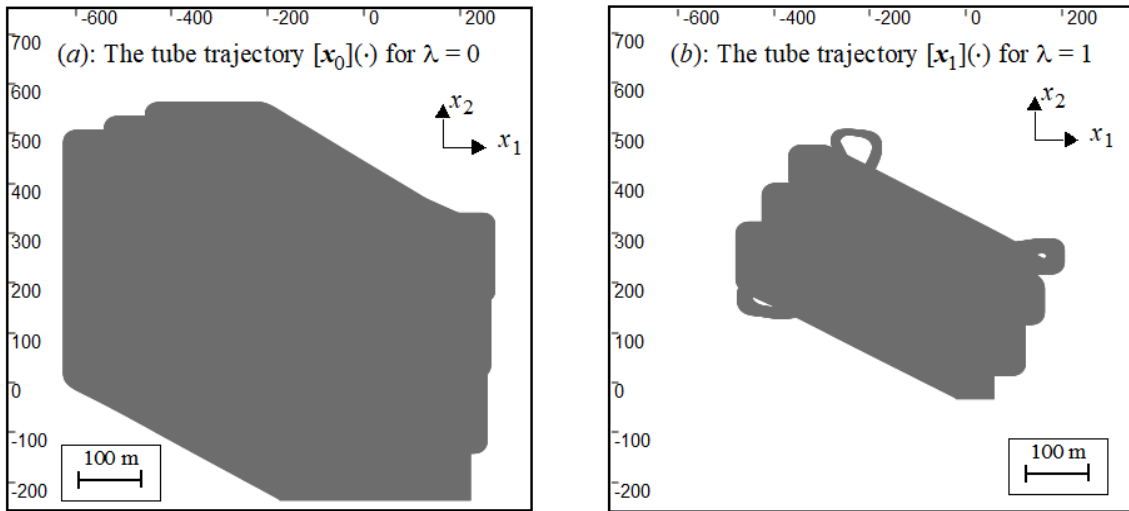


Fig. 38. Daurade tube trajectories due to the speed and heading drifts.

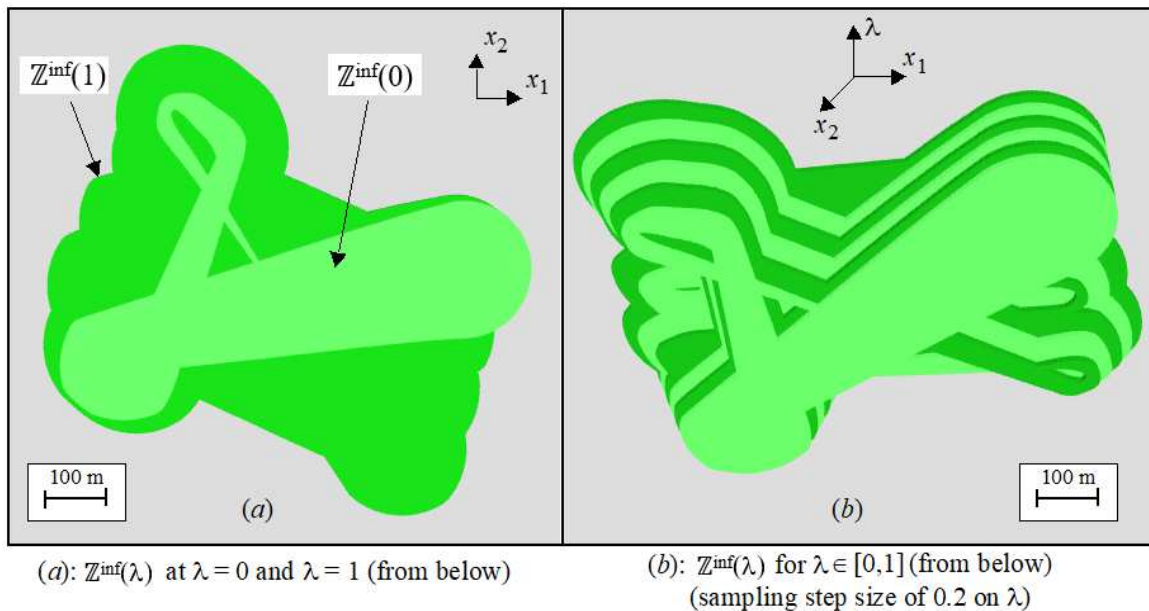


Fig. 39. Representation of $Z^{\text{inf}}(\lambda)$.

For example, masses of belief $m(Z^{\text{inf}}(\lambda_i))$ can be associated with $Z^{\text{inf}}(\lambda_i)$, $\lambda_i \in [0, 1]$, which are considered as focal elements. In this case, for a degree λ_i , the belief function (*Bel*) represents the sum of the masses that necessarily imply $Z^{\text{inf}}(\lambda)$. The plausibility measure (*Pl*) refers to the sum of the masses that do not necessarily contradict $Z^{\text{inf}}(\lambda)$. The *Bel* measure evaluates up to what extent it is certain that the information represented by $m(Z^{\text{inf}}(\lambda_i))$ implies that a point in the seafloor $\in Z^{\text{inf}}(\lambda)$. The *Pl* measure evaluates up to what extent the information represented by mass $m(Z^{\text{inf}}(\lambda_i))$ does not contradict the proposition: a point in the seafloor $\in Z^{\text{inf}}(\lambda)$. In this case, for a given level λ_i , the safety probability of $Z^{\text{inf}}(\lambda)$ is in the interval bounded by the *Bel* and *Pl* measures. The same reasoning can be used on $Z^{\text{sup}}(\lambda)$. For more details, see [7] on how uncertainty is quantified using the possibility and belief-function theories in a gradual context.

5 Conclusion

In this paper, a new concept of TGSs is proposed. A TGS originates from the GS and TS concepts. TGS $\llbracket X(\lambda) \rrbracket = \llbracket X^{\text{inf}}(\lambda), X^{\text{sup}}(\lambda) \rrbracket$ is an interval of GSs, which is delimited by two lower

$\mathbb{X}^{\text{inf}}(\lambda)$ and upper $\mathbb{X}^{\text{sup}}(\lambda)$ GS bounds. One originality of this approach is that it can represent uncertain quantities that are not easily represented by CSs, T1FSs, GSs, and/or T2FSs. Another originality is the provision of a new representation of uncertain GSs. Furthermore, logical and arithmetical operations on uncertain GSs can be implemented using the TGS formalism. The potential applicability of this approach has been validated using application examples in solving fuzzy SoEs, fuzzy regression contexts, and real-world application using an underwater robot. Furthermore, the proposed method can be applied to more complex real-world applications in several domains such as in uncertain linear and nonlinear control and uncertain linear and nonlinear optimization problems, among others. In their philosophy of representation, GSs and TGS are linked to T1FSs [20] and T2FSs [45][50], respectively. Therefore, under some conditions, a GS can be considered as a T1FS. Similarly, a TGS can be considered as a particular case of a T2FS. In a short term, work will be devoted to a deep analysis and comparison between TGS and T2FSs. Therefore, from the methodological perspectives, the TGS and T2FS concepts are not contrary but rather complementary. Another interesting objective is to deploy TSs and TGSs in fuzzy optimization problems, synthesis of uncertain controllers, and stability study of control structures. For instance, by assuming a dynamical system, if we consider a controller and a Lyapunov function to study the stability of a closed control loop, we can possibly quantify the zones of instability, certain stability, and plausible stability. In the long term, we will focus on the development of methodologies that are capable of explaining existing links between multigranulation rough sets [42], T2FSs, and TGSs so that they can be integrated to solve complex learning, decision, and control problems. In this context, special attention will be provided to fuzzy and gradual deep-learning methods. To achieve more accurate results, this perspective will require a decade of research and development.

References

- [1] Acharjya D.P., Abraham A., Rough computing — A review of abstraction, hybridization and extent of applications, *Engineering Applications of Artificial Intelligence*, Vol. 96, 103924, 2020.
- [2] Allahviranloo T., Ghanbari M., Hosseinzadeh A.A., Haghi E., Nuraei R., A note on ‘fuzzy linear systems’, *Fuzzy Sets and Systems*, Vol. 177, pp. 87–92., 2011.
- [3] Allahviranloo T., Ghanbari M., On the algebraic solution of fuzzy linear systems based on interval theory, *Appl. Math. Model*, Vol 36 (11), pp. 5360–5379, 2012.
- [4] Bissierier A., Boukezzoula R., Galichet S., A Revisited Approach for Linear Fuzzy Regression Using Trapezoidal Fuzzy Intervals, *Information Sciences*, Vol. 180, N°19, pp. 3653-3673, 2010.
- [5] Boukezzoula R., Coquin D., A decision-making computational methodology for a class of type-2 fuzzy intervals: An interval-based approach, *Information Sciences*, Vol. 510, pp. 256-282, 2020.
- [6] Boukezzoula R., Jaulin L. and Foulloy L., Thick gradual intervals: An alternative interpretation of type-2 fuzzy intervals and its potential use in type-2 fuzzy computations, *Engineering Applications of Artificial Intelligence*, vol. 85, pp. 691-712, 2019.
- [7] Boukezzoula R., Galichet S. and Coquin D., From fuzzy regression to gradual regression: Interval-based analysis and extensions, *Information Sciences*, Vol. 441, pp. 18-40, 2018.
- [8] Boukezzoula R., Galichet S., Foulloy L., Elmasry M., Extended gradual interval (EGI) arithmetic and its application to gradual weighted averages, *Fuzzy Sets and Systems*, Vol. 257, pp. 67-84, 2014.
- [9] Boukezzoula R., Galichet S., Bissierier A., A Midpoint–Radius approach to regression with interval data, *International Journal of Approx. Reason.*, Vol. 52, N° 9, pp. 1257-1271, 2011.
- [10] Castillo O., Amador-Angulo L., Castro J-R., Garcia-Valdez M., A comparative study of type-1 fuzzy logic systems, interval type-2 fuzzy logic systems and generalized type-2 fuzzy logic systems in control problems, *Information Sciences*, Vol. 354, pp. 257-274, 2016.
- [11] Castillo O., Cervantes L., Soria J., Sanchez M., Castro J-R. (2016b), Generalized type-2 fuzzy granular approach with applications to aerospace, *Information Sciences*, Vol. 354, pp. 165–177, 2016.
- [12] Castillo O., Melin P., *Type-2 Fuzzy Logic Theory and Applications*, Springer-Verlag, Berlin, 2008.
- [13] Cerny M. and Hladik M., Possibilistic linear regression with fuzzy data: Tolerance approach with prior information, *Fuzzy Sets & Syst.*, Vol. 304, pp. 127-144, 2018.
- [14] Chabert G. and Jaulin L., Contractor programming, *Artificial Intell.*, Vol. 173, pp. 1079-1100, 2009.
- [15] Chen L-H., Nien S-H., A new approach to formulate fuzzy regression models, *Appl. Soft Comp. J.*, Vol. 86, pp. 1-10, 2020.

- [16] Chuang C.C., Extended support vector interval regression networks for interval input–output data, *Inform. Sci.*, Vol. 178, pp. 871–891, 2008.
- [17] Chukhrova N., Johannssen A., Fuzzy regression analysis: Systematic review and bibliography, *Applied Soft Computing*, Vol. 84, pp. 1-29, 2019.
- [18] Desrochers B., and Jaulin L., Thick set inversion, *Artificial Intelligence*, Vol. 249, pp. 1-18, 2017.
- [19] Desrochers B., Simultaneous Localization and Mapping in Unstructured Environments, A Set-Membership Approach, PhD thesis, ENSTA Bretagne, France, 2018.
- [20] Dubois D. and Prade H., Gradual elements in a fuzzy set, *Soft Computing*, No. 12, pp. 165-175, 2008.
- [21] Diamond P., Fuzzy Least Squares, *Information Sciences*, Vol. 46. pp. 141-157, 1988.
- [22] Dubois D., Kerre E., Mesiar R., Prade H., Fuzzy interval analysis, in: D. Dubois, H. Prade (Eds.), *Fundamentals of Fuzzy Sets*, The Handbooks of Fuzzy Sets Series, Kluwer, Boston, pp. 483–581, 2000.
- [23] D’Urso P. and Gastaldi T., A least-squares approach to fuzzy linear regression analysis, *Comp. Stat. & Data Anal.*, 34, pp. 427-440, 2000.
- [24] Dymova L., Sevastjanov P., Tikhonenko A., An interval type-2 fuzzy extension of the TOPSIS method using alpha-cuts, *Knowledge-Based Systems*, Vol. 83, pp.116–127, 2015.
- [25] Dymova L., Sevastjanov P., Pilarek M., A method for solving systems of linear interval equations applied to the Leontief input–output model of economics, *Expert Systems with Applications*, Vol. 40, pp. 222-230, 2013.
- [26] Figueroa-Garcia J-C., Chalco-Cano Y., Roman-Flores H., Distance measures for Interval Type-2 fuzzy numbers, *Discrete Applied Mathematics*, Vol. 197, pp. 93–102, 2015.
- [27] Fortin J., Dubois D. and Fargier H., Gradual numbers and their application to fuzzy interval analysis, *IEEE Trans. on Fuzzy Syst.*, Vol. 16 (2), pp. 388-402, 2008.
- [28] Friedman M., Ming M., Kandel A., Fuzzy linear systems, *Fuzzy Sets and Systems*, Vol. 96, pp. 201–209, 1998.
- [29] Golsefid S-M., Zarandi M-H., Turksen I-B., Multi-central general type-2 fuzzy clustering approach for pattern recognition, *Information Sciences*, Vol. 328, pp. 172–188, 2016.
- [30] Hamrawi H., Coupland S., John R., Type-2 Fuzzy Alpha-Cuts, *IEEE Trans. on Fuzzy Syst.*, Vol 25(3): pp. 682-692, 2017.
- [31] Horcik R., Solution of a system of linear equations with fuzzy numbers, *Fuzzy Sets and Systems*, Vol. 159, pp. 1788–1810, 2008.
- [32] Huang Z., Zhu D., Sun B., A multi-AUV cooperative hunting method in 3-D underwater environment with obstacle, *Engineering Applications of Artificial Intelligence*, Vol. 50, pp. 192-200, 2016.
- [33] Jaulin L., Braems I. and Walter E., Interval methods for nonlinear identification and robust control, In *Proc. of the 41st IEEE Conference on Decision and Control*, Las Vegas, Vol. 4, pp. 4676-4681, 2002.
- [34] Jaulin L., Solving set-valued constraint satisfaction problems, *Computing*, Vol. 94 (2), pp. 297-311, 2012.
- [35] Kaucher E., Interval analysis in the extended interval space \mathbb{IR} , *Computing, Suppl.*, Vol. 2, pp. 33–49, 1980.
- [36] Keyanpour M., Mohaghegh Tabar M., Lodwick W., Solution Algorithm for a System of Interval Linear Equations Based on the Constraint Interval Point of View, *Reliable Computing*, Vol. 26, pp. 1-12, 2018.
- [37] Kleene S.C., Introduction to metamathematics, North-Holland, Amsterdam, 1952.
- [38] Landowski M., Method with horizontal fuzzy numbers for solving real fuzzy linear systems, *Soft Computing*, Vol. 23, pp. 3921-3933, 2019.
- [39] Liu P., Jin F., A multi-attribute group decision-making method based on weighted geometric aggregation operators of interval-valued trapezoidal fuzzy numbers, *Applied Math. Modelling*, Vol. 36(6), pp. 2498–2509, 2012.
- [40] Lodwick W.A. and Dubois D., Interval linear systems as a necessary step in fuzzy linear systems, *Fuzzy Sets and Systems*, Vol. 281, pp. 227-251, 2015.
- [41] Lopez-Maestresalas A., De Miguel L., Lopez-Molina C., Arazuri S, Bustince H., Jaren C., Hyperspectral imaging using notions from type-2 fuzzy sets, *Soft Computing*, Vol. 23, pp. 1779–1793, 2019.
- [42] Lu J., Type-2 fuzzy multigranulation rough sets, *Int. Journal of Appr. Reas.*, Vol. 124, pp. 173–193, 2020.
- [43] Malinowski G., Kleene logic and inference, *Bull Sect. Logic* Vol. 43(1/2), pp. 43–52, 2014.
- [44] Melin P., Ontiveros-Robles E., Gonzalez C-I., Castro J-R., Castillo O., An approach for parameterized shadowed type-2 fuzzy membership functions applied in control applications, *Soft Computing*, Vol. 23, pp. 3887–3901, 2019.
- [45] Mendel J.M., Uncertain Rule-Based Fuzzy Logic Systems: Introduction and New Directions. Upper Saddle River, NJ: Prentice-Hall, 2001.
- [46] Mendel J.M. and Bob John R.I., Type-2 Fuzzy Sets Made Simple, *IEEE Transactions on Fuzzy Systems*, Vol. 10(2), pp. 117-127, 2002.
- [47] Mendel J-M., Hagrass H., Bustince H., Herrera F., Comments on “Interval Type-2 Fuzzy Sets are Generalization of Interval-Valued Fuzzy Sets: Towards a Wide View on Their Relationship”, *IEEE Trans. on Fuzzy Syst.*, Vol. 24(1), pp. 249-250, 2016.
- [48] Mendel J-M., Liu F., Zhai D., α -Plane Representation for Type-2 Fuzzy Sets: Theory and Applications, *IEEE Trans. on Fuzzy Syst.*, Vol. 17(5), pp. 1189-1207, 2009.

- [49] Mendel J-M., John R-I., Liu F., Interval type-2 fuzzy logic systems made simple, *IEEE Trans. Fuzzy Syst.*, Vol. 14(6), pp. 808-821, 2006.
- [50] Mittal K., Jain A., Vaislac K-S., Castillo O., Kacprzyke J., A comprehensive review on type 2 fuzzy logic applications: Past, present and future, *Engineering Applications of Artificial Intelligence*, Vol. 95, 103916, 2020.
- [51] Mo H., Wang F.Y., Zhou M., Li R., Xiao Z., Footprint of uncertainty for type-2 fuzzy sets, *Information Sciences*, pp. 96-110, Vol. 272, 2014.
- [52] Mohaghegh Tabar M., Keyanpour M., Lodwick W.A., Solving interval linear programming problems with equality constraints using extended interval enclosure solutions, *Soft Computing*, Vol. 23, pp. 7439–7449, 2019.
- [53] Negoita, C.V. and Ralescu, D.A., *Applications of Fuzzy Sets to Systems Analysis*, Wiley, New York, 1975.
- [54] Pawlak Z., Rough sets, *Int. J. Comput. Inf. Sci.*, vol. 11 (5), pp. 341-356, 1982.
- [55] Pawlak Z., *Rough Sets: Theoretical Aspects of Reasoning About Data*. Kluwer Acad. Publ., Norwell, MA, USA.
- [56] Popova E.D., Hladík M., Outer enclosures to the parametric AE solution set, *Soft Comput.*, Vol. 17(8), pp. 1403–1414, 2013.
- [57] Qin J., Liu X., Pedrycz W., A multiple attribute interval type-2 fuzzy group decision making and its application to supplier selection with extended LINMAP method, *Soft Computing*, Vol. 21, pp. 3207–3226, 2017.
- [58] Ralescu D.A., A generalization of the representation theorem, *Fuzzy Sets and Systems*, Vol. 51, pp. 309-311, 1992.
- [59] Runkler T., Coupland S., John R., Interval type-2 fuzzy decision making, *Int. Journal of App. Reas.*, Vol. 80, pp. 217-224, 2017.
- [60] Rohou S., Jaulin L., Mihaylova M., Le Bars F., Veres S., Guaranteed Computation of Robots Trajectories, *Robotics and Autonomous Systems*, Vol. 93, pp.76–84, 2017.
- [61] Rzezuchowski T., Wasowski J., Solutions of fuzzy equations based on Kaucher arithmetic and AE-solution sets, *Fuzzy sets and Systems*, Vol. 159, 2116 – 2129, 2008.
- [62] Sevastjanov P., Dymova L., A new method for solving interval and fuzzy equations: linear case, *Information Sci.*, Vol. 179, pp. 925–937, 2009.
- [63] Shary S.P., A New Technique in Systems Analysis under Interval Uncertainty and Ambiguity, *Reliable Computing*, Vol. 8, pp. 321–418, 2002.
- [64] Shary S.P., Outer Estimation of Generalized Solution Sets to Interval Linear Systems, *Reliable Computing*, Vol. 5, pp. 323-335, 1999.
- [65] Shary S.P., An Interval Linear Tolerance Problem, *Aut. and Remote Control*, Vol. 65 (10), pp. 1653–1666, 2004.
- [66] Shary S. P., Weak and Strong Compatibility in Data Fitting Problems Under Interval Uncertainty. *Advances in data science and adaptive analysis*, Vol. 12(1), [2050002], 2020.
- [67] Suo C., Li Y., Li Z., On n-polygonal interval-value fuzzy sets and numbers, *Fuzzy sets and Systems*, 2020, doi.org/10.1016/j.fss.2020.10.014.
- [68] Tanaka H. and Ishibushi H., Identification of possibilistic linear systems by quadratic membership functions of fuzzy parameters, *Fuzzy Sets & Syst.* 41, pp. 145-160, 1991.
- [69] Tolga A.C., Parlak I.B., Castillo O., Finite-interval-valued Type-2 Gaussian fuzzy numbers applied to fuzzy TODIM in a healthcare problem, *Engineering Applications of Artificial Intelligence*, Vol. 87, 103352, 2020.
- [70] Torres-Blanc C., Cubillo S., Hernández P., Aggregation operators on type-2 fuzzy sets, *Fuzzy Sets & Syst.*, Vol. 324, pp. 74–90, 2017.
- [71] Wu D., Mendel J-M., Aggregation Using the Linguistic Weighted Average and Interval Type-2 Fuzzy Sets, *IEEE Trans. on Fuzzy Syst.*, Vol 15(6), pp. 1145-1161, 2007.
- [72] Wu D., Mendel J.M., Recommendations on designing practical interval type-2 fuzzy systems, *Engineering Applications of Artificial Intelligence*, Vol. 85, pp. 182-193, 2019.
- [73] Zhang Q., Xie Q. and Wang G., A survey on rough set theory and its applications, *CAAI Transactions on Intelligence Technology*, Vol. 1, N° 4, pp. 323-333, 2016.